Renewable and Sustainable Energy Reviews 194 (2024) 114314

Contents lists available at ScienceDirect

Renewable and Sustainable Energy Reviews

journal homepage: www.elsevier.com/locate/rser

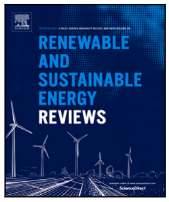

Original research article

Near-term infrastructure rollout and investment strategies for net-zero hydrogen supply chains

Alissa Ganter [a], Paolo Gabrielli [a,b], Giovanni Sansavini [a,*]

[a] Institute of Energy and Process Engineering, ETH Zurich, Zurich, 8092, Switzerland
[b] Department of Global Ecology, Carnegie Institution for Science, Stanford, 94305, CA, USA

ARTICLE INFO

Dataset link: https://doi.org/10.5281/zenodo.10568836

Keywords:
Net-zero emissions
Hydrogen production
European hydrogen infrastructure
Hard-to-abate industries
Decarbonization pathways
Optimization

ABSTRACT

Low-carbon hydrogen plays a key role in European industrial decarbonization strategies. This work investigates the cost-optimal planning of European low-carbon hydrogen supply chains in the near term (2025–2035), comparing several hydrogen production technologies and considering multiple spatial scales. We focus on mature hydrogen production technologies: steam methane reforming of natural gas, biomethane reforming, biomass gasification, and water electrolysis. The analysis includes carbon capture and storage for natural gas and biomass-derived hydrogen. We formulate and solve a linear optimization model that determines the cost-optimal type, size, and location of hydrogen production and transport technologies in compliance with selected carbon emission targets, including the EU fit for 55 target and an ambitious net-zero emissions target for 2035. Existing steam methane reforming capacities are considered, and optimal carbon and biomass networks are designed. Findings identify biomass-based hydrogen production as the most cost-efficient hydrogen technology. Carbon capture and storage is installed to achieve net-zero carbon emissions, while electrolysis remains cost-disadvantageous and is deployed on a limited scale across all considered sensitivity scenarios. Our analysis highlights the importance of spatial resolution, revealing that national perspectives underestimate costs by neglecting domestic transport needs and regional resource constraints, emphasizing the necessity for highly decarbonized infrastructure designs aligned with renewable resource availabilities.

1. Introduction

Hydrogen plays a central role in the decarbonization strategy of the European Union (EU) as it has the potential to decarbonize a range of sectors [1,2]. These sectors include so-called hard-to-abate sectors where it is proving difficult to meaningfully reduce greenhouse gas (GHG) emissions due to the lack of cost-competitive solutions and the need to use hydrogen as a feedstock as well as an energy source [3,4]. In 2020, about 309 TWh (9.3 Mt) of hydrogen were consumed in Europe [5]. Major consumers were two hard-to-abate industries, namely refineries (47%) and the chemical industry (45%), where hydrogen is required as feedstock to produce ammonia, methanol, and other chemicals (e.g., polymers, and polyurethanes) [5,6].

Currently, hydrogen is predominantly produced from natural gas via steam methane reforming (SMR) [7], contributing to about 4 % of the European GHG emissions [8]. Hence, a switch to hydrogen produced with low-carbon emissions is required. In Europe, hydrogen is considered "low-carbon" if process emissions remain below 131 kg_{CO_2}/MWh_{H_2} (3.9 kg_{CO_2}/kg_{H_2}) [9]. Previous studies suggest that the potential of renewable energy sources in Europe is sufficient to produce low-carbon hydrogen and decarbonize the chemical industry and refineries [10,11].

However, the existing low-carbon hydrogen production capacity in Europe is small (about 1.75 GW_{H_2}) [12], and only small-scale, local hydrogen networks exist (about 125 km), which supply chemical industry in Belgium, the Netherlands, and Germany [13]. To scale up low-carbon hydrogen demand and supply, and enable its widespread use, the EU envisions a large-scale European hydrogen supply chain [14]. However, uncertainty surrounding future low-carbon hydrogen demands, supply, and infrastructure hamper their proliferation. This situation is also referred to as the three-sided "chicken-and-egg" problem [15], where the lack of demand hinders investments in supply technologies, and the lack of supply hinders investments in transport infrastructure. Solving this problem requires a coordinated scale-up of low-carbon hydrogen demand, supply, and transport infrastructure. So far, existing scientific literature offers divergent views on whether such a European hydrogen supply chain infrastructure is required: While some suggest small-scale, regional supply chains [16], others call for a large-scale European supply chain [17–19]. In addition, a comparative assessment of the

* Corresponding author.
E-mail address: sansavig@ethz.ch (G. Sansavini).

https://doi.org/10.1016/j.rser.2024.114314
Received 18 April 2023; Received in revised form 31 January 2024; Accepted 31 January 2024
Available online 14 February 2024

Abbreviations

EU	European Union
CCS	Carbon capture and storage
GHG	Greenhouse gas
HSC	Hydrogen supply chain
LCOE	Levelized cost of energy
LCOH	Levelized cost of hydrogen
NUTS	Nomenclature of territorial units for statistics
SMR	Steam methane reforming

Nomenclature of the Optimization Problem

Sets	**Description**
$\mathcal{C}$	Set of carriers
$\mathcal{H}$	Set of technologies
$\mathcal{P}$	Set of positions (nodes and edges)
$\mathcal{M}$	Set of countries
$\mathcal{T}$	set of time steps
Subsets	**Description**
$\mathcal{C}^{\text{imp}} \subseteq \mathcal{C}$	Set of import carriers
$\mathcal{C}^{\text{exp}} \subseteq \mathcal{C}$	Set of export carriers
$\mathcal{I} \subseteq \mathcal{H}$	Set of conversion technologies
$\mathcal{I}^{\text{Cond}} \subseteq \mathcal{I}$	Set of conditioning technologies
$\mathcal{J} \subseteq \mathcal{H}$	Set of transport technologies
$\mathcal{N} \subseteq \mathcal{L}$	Set of nodes
$\mathcal{E} \subseteq \mathcal{L}$	Set of edges
Indexed Sets	**Description**
$\mathcal{N}_m^{\text{C}} \subseteq \mathcal{N}$	Set of nodes within country m
$\underline{\mathcal{E}}_n \subseteq \mathcal{E}$	Set of ingoing edges for node n
$\overline{\mathcal{E}}_n \subseteq \mathcal{E}$	Set of outgoing edges for node n
$\mathcal{C}_h^{\text{r}} = \{c_h^{\text{r}}\} \subseteq \mathcal{C}$	Set of reference carrier for technology $h \in \mathcal{H}$
$\underline{\mathcal{C}}_h \subseteq \mathcal{C}$	Set of input carriers for conversion technology $h \in \mathcal{J}$
$\overline{\mathcal{C}}_h \subseteq \mathcal{C}$	Set of output carriers for conversion technology $h \in \mathcal{J}$
Parameter	**Description**
$d_{c,n,t}$	Demand of carrier c at node n and tim t
$\underline{u}_{c,n,t}$	Import price of carrier $c \in \mathcal{C}^{\text{imp}}$ at node n and time t
$\overline{u}_{c,n,t}$	Export price of carrier $c \in \mathcal{C}^{\text{exp}}$ at node n and time t
$a_{c,n,t}$	Availability of carrier c at node n and time t
$s_{h,p,\bar{t}}^{\text{ex}}$	Existing capacity of technology h at position p built at time $\bar{t} \in [-l_h, 0]$
$s_{h,p}^{\max}$	Maximum capacity of technology h at position p
$\Delta s_h^{\max}$	Maximum capacity increase of technology h
$s_{h,m,t}^{\lim}$	Capacity of hydrogen production technology h in country m at time t
l_h	Lifetime of technology h
$\eta_{h,c,c'}$	Conversion efficiency of conversion technology $h \in \mathcal{I}$ for input carrier c and output carrier c'
$\lambda_{h,e}$	Transport distance of edge e for transport technology $h \in \mathcal{J}$
ρ_h	Loss coefficient for transport technology $h \in \mathcal{J}$
e_t	Carbon emission limit at time t
e_t^{o}	Carbon emission overshoot at time t
μ^{o}	Carbon emission overshoot price
ϵ_c, ϵ_h	Carbon intensity of carrier c and technology h
r	Discount rate
α_h	Capital unit cost of technology h
$\hat{\alpha}_h$	Capital unit cost per distance of transport technology $h \in \mathcal{J}$
β_h	Variable operational unit cost of technology h
$\hat{\beta}_h$	Variable operational unit cost per distance of transport technology $h \in \mathcal{J}$
γ_h	Fixed operational unit cost of technology h
$\hat{\gamma}_h$	Fix operational unit cost per distance of transport technology $h \in \mathcal{J}$
Variable	**Description**
$S_{h,p,t}$	Capacity of technology h at position p and time t
$\Delta S_{h,p,t}$	Capacity increase of technology h at position p and time t
$\underline{G}_{c,h,n,t}$	Input flow of carrier $c \in \underline{\mathcal{C}}_i$ into conversion technology $h \in \mathcal{I}$ at node n and time t
$\overline{G}_{c,h,n,t}$	Output flow of carrier $c \in \overline{\mathcal{C}}_i$ from conversion technology $h \in \mathcal{I}$ at node n and time t
$F_{c,h,e,t}$	Flow of carrier c through transport technology $h \in \mathcal{J}$ at edge e and time t
$F_{c,h,e,t}^{\text{l}}$	Loss of carrier c through transport technology $h \in \mathcal{J}$ at edge $e \in \mathcal{E}$ and time t
$\underline{U}_{c,n,t}$	Import of carrier $c \in \mathcal{C}^{\text{imp}}$ at node n and time t
$\overline{U}_{c,n,t}$	Export of carrier $c \in \mathcal{C}^{\text{exp}}$ at node $n \in \mathcal{N}$ and time t
NPC	Net present cost
CAPEX_t	Capital expenditures at time t
OPEX_t	Operational expenditures at time t

different low-carbon hydrogen production pathways and the coupling with carbon and biomass supply chains is missing.

One reason for these inconclusive findings is the lack of a comprehensive modeling and optimization framework with a sufficient spatial resolution that captures the evolution of hydrogen supply chains over multi-year time horizons and allows the combined assessment of different low-carbon hydrogen production pathways, as well as the coupling with carbon and biomass supply chains. We aim to fill this gap by (i) analyzing the hydrogen supply chain infrastructure requirements that can support the widespread use of low-carbon hydrogen in Europe in the near term, (ii) determining synergies and trade-offs between the production, use, and transport of hydrogen, carbon, and biomass, (iii) assessing the impact of spatial resolution on the optimal infrastructure design, and (iv) identifying the spatial resolution required to support the decision-making process and provide clear design recommendations.

1.1. Low-carbon hydrogen production pathways

Hydrogen can be produced starting from several feedstocks and energy sources, including natural gas, electricity, and biomass [20]. Hydrogen production from natural gas via SMR is currently considered

Table 1
Levelized cost of hydrogen (LCOH) and carbon intensity of the different hydrogen production pathways based on [20,21,26,28,31,32]. SMR: Steam methane reforming. CCS: Carbon capture and storage.

Production pathway	LCOH [€/kg_{H_2}]	Carbon intensity [kg_{CO_2}/kg_{H_2}]
Natural gas SMR	0.7 – 1.9	10.0 – 17.2
Natural gas SMR-CCS	1.1 – 2.5	2.97– 9.2
Biomethane SMR	1.6 – 2.1	−9.6 – 8.6
Biomethane SMR-CCS	1.9 – 2.8[a]	−13.6 – −6
Biomass gasification	1.3 – 2.7	0.3 – 8.6
Biomass gasification-CCS	2.0 – 3.2	−17.5 – −11.7
Electrolysis wind/solar	2.9 – 13.2	0.41 – 7.1

[a] Assuming CCS increases hydrogen production cost by 15–30 % [33].

the most cost-efficient hydrogen production pathway [21]. However, SMR from natural gas is associated with large carbon emissions [20]. To reduce process emissions, SMR can be coupled with carbon capture and storage (CCS). Carbon capture rates of 90 % or more are required such that the process can be considered "low-carbon" [22]. From the set of currently available low-carbon hydrogen production pathways, SMR coupled with CCS is considered one of the most cost-efficient low-carbon hydrogen production pathways [23].

Alternatively, low-carbon hydrogen can be produced from renewable energy sources. Mature hydrogen production technologies are (i) water electrolysis from renewable electricity, (ii) biomass gasification, and (iii) biomethane reforming [2]. Table 1 provides an overview of the cost and emissions associated with the different hydrogen production pathways. While water electrolysis from renewable electricity is associated with low process emissions [20], it is significantly more expensive than SMR with CCS (+5 €/kg) and biomass-based hydrogen production pathways (+4.7 €/kg) [24]. Although renewable electricity prices continuously decrease, water-electrolysis is not expected to become cost-competitive before 2030 [24,25].

Recent evidence suggests biomass-based hydrogen production routes as economically and environmentally attractive alternatives to fossil-fuel-based hydrogen production routes (Table 1) [21]. Furthermore, by coupling biomass-based hydrogen production with CCS, net-negative process emissions are achieved [26,27], which can generate the carbon removal needed to decarbonize the chemical industry and refineries in Europe [28]. However, combined assessments of the required hydrogen and carbon supply chain infrastructure are rare thus far [23,29,30].

Although a large selection of low-carbon hydrogen production technologies exists, most studies that are performed at the continental scale focus their assessment on low-carbon hydrogen production from renewable electricity via water electrolysis and SMR-CCS [16,18,34]. However, several studies that do consider multiple low-carbon hydrogen production technologies indicate biomass-based hydrogen production as a cost-efficient low-carbon hydrogen production technology [23,35,36].

So far, a continental-scale comparative assessment of the different low-carbon hydrogen production pathways is missing. Moreover, an integrated system perspective can provide insights into the interplay between the supply chains [37]. Here, we aim to address this gap and include a selection of mature hydrogen production pathways in our assessment to analyze the synergies and trade-offs between the different hydrogen production pathways and supply chains.

1.2. Optimal design of hydrogen supply chains: Geographical coverage and spatial resolution

In general, hydrogen supply chains (HSCs) can be defined as a network of hydrogen production and consumption sites interconnected by hydrogen transport options. Several optimization-based models exist to design and operate HSCs for single and multiple periods [38–40]. While single-period models present a snapshot in time, multi-period models capture the optimal evolution of the HSC design over long planning horizons and allow the identification of challenges during the transition [41].

The optimal design of HSCs has been investigated via single- and multi-objective optimization, considering system cost, global warming potential, and safety risks [42]. Moreover, the risk and robustness of the supply chain designs has been addressed [43,44]; and the influence of the uncertainty of relevant input parameters, such as the hydrogen demand, is investigated [45,46]. Besides hydrogen demand, investment cost and gas prices are identified as critical factors affecting the supply chain infrastructure rollout [47].

The geographical coverage and spatial resolution vary greatly across HSC studies. Many regional and national hydrogen supply chain models exist [37]. In comparison, continental-scale hydrogen supply chain models are less common, and only a few optimization-based models exist [18,34]. Regional models are typically able to include higher levels of detail due to their smaller geographical coverage. However, regional models cannot capture cross-regional synergies, which can result in sub-optimal solutions [36,48].

Besides the geographical coverage, spatial resolution is identified as a crucial determinant of infrastructure designs [49–51]. A comparison of different energy system models with varying spatial resolutions shows that the level of spatial resolution can significantly impact the results [50]. In general, optimization models with high spatial resolution can capture spatially variable input data with higher accuracy [52]. However, highly-resolved optimization problems can quickly become computationally intractable [53]. To manage computational limitations and maintain tractability, the complexity of the optimization problem has to be reduced. This requires trade-offs, e.g., with respect to the level of temporal resolution, spatial resolution, and geographical coverage. In this context, time series aggregation methods are an effective tool to reduce the temporal resolution of the optimization problem by grouping similar time steps [54,55]. [56] compare available time series aggregation methods and discuss their impact on the results.

Several studies investigate the impact of different levels of spatial resolutions for the heating sector [49,50], and the power sector [57–60]. In particular for systems with high shares of renewable energy sources and heterogeneous renewable energy potentials, selecting a sufficient spatial resolution is key. However, no direct relationship has been established between the required level of spatial resolution and the share of renewable energy sources thus far. Instead, it is suggested to investigate the impact of spatial resolution on the model results depending on the specific application [50].

To date, no comprehensive analysis of the impact of spatial resolution on the optimal design and infrastructure rollout of HSCs exists. We aim to address this gap and investigate the impact of spatial resolution on the optimal infrastructure design to identify the spatial resolution required to provide clear design recommendations and support the decision-making process.

1.3. Scope of the work and structure of the paper

This contribution determines optimal pathways to decarbonize the hydrogen supply for the chemical industry and refineries, and enable the widespread use of low-carbon hydrogen in Europe in the near term (2025–2035). We perform a comparative assessment of low-carbon hydrogen production pathways and determine the level of spatial resolution required to reliably design hydrogen supply chains (HSCs) and support robust decision-making. To investigate the impact of spatial resolution, we determine the optimal HSC design for two levels of spatial resolution, namely regional and national, and compare the levelized cost of hydrogen, the optimal investment strategies, and the network structures of the hydrogen, carbon, and biomass supply chains. A multi-year time horizon is considered to model the transition from 2025 until 2035, where hydrogen is predominantly produced on-site from natural gas via SMR, to a system where hydrogen is produced with low-carbon emissions.

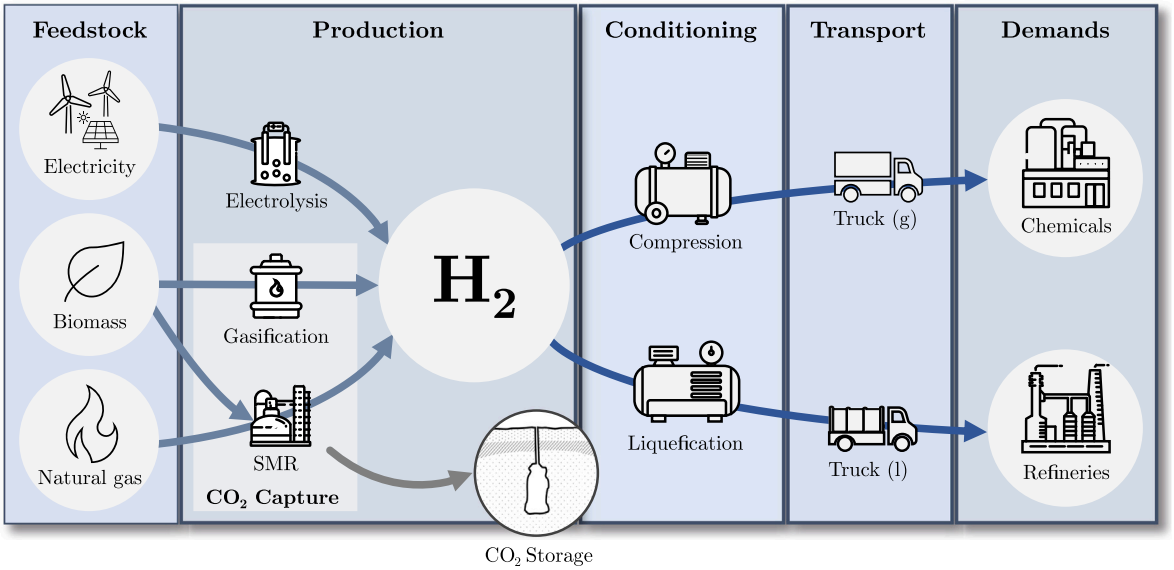

Fig. 1. Overview of the hydrogen supply chain components: Available feedstocks, hydrogen production technologies, conditioning technologies, hydrogen transport options, and the considered hydrogen demand sources.

An optimization-based HSC model is developed to determine the optimal infrastructure rollout from 2025 to 2035. A carbon supply chain is designed alongside the HSC to investigate the coupling of hydrogen production with CCS. In addition, biomass transport is considered, and a biomass supply chain is designed, allowing us to analyze the synergies and trade-offs between hydrogen, carbon, and biomass supply chains. We focus on commercially available technologies to identify near-term solutions that can kick-start the development and deployment of low-carbon hydrogen and carbon supply chains.

The paper is structured as follows. Section 2 describes the system configuration and supply chains. Section 3 formulates the optimization problem. Section 4 presents the optimal design of the HSCs and analyzes the impact of spatial resolution. Finally, Section 5 discusses the findings, and Section 6 concludes.

2. Low-carbon hydrogen supply chain

Fig. 1 illustrates the HSC. Starting from the available feedstocks and energy sources, hydrogen is produced, conditioned, and transported to the consumption sites. The HSC is modeled as a network of nodes, which are connected by edges. In the regional model, the nodes represent NUTS2 regions [61]; in the national model, the nodes represent countries. The production, conditioning, and transport technologies, as well as natural gas and grid-electricity, are assumed to be available at all nodes of the supply chain. In contrast, the renewable energy sources, wind, solar, and biomass, are limited by the available potential (Fig. 2).

In the following, the hydrogen, carbon, and biomass supply chains are described in more detail. The input data is available as Supporting Information and published as part of the data repository on Zenodo [62].

2.1. Feedstocks and energy sources for hydrogen production

The available feedstocks and energy sources for hydrogen production are electricity, natural gas, and biomass. We assume that grid electricity and natural gas are available at each node of the supply chain. The country-specific electricity and natural gas prices are taken from [63,64], and the yearly evolution of the electricity, the natural gas prices, and the country-specific electricity grid carbon intensities are derived from [63]. In addition, renewable electricity can be generated from wind (about 6500 TWh) and solar energy (about 1000 TWh) according to the available technical potentials in each region (Fig. 2). The regional- and time-dependent technical potentials for wind and solar energy are taken from [65,66]. The remaining techno-economic parameters of the renewable energy technologies are based on [67,68].

Besides wind and solar energy, biomass is considered as a renewable energy resource. The biomass availability is limited by the technical potential, which describes the maximum accessible wet and dry biomass availability, considering technical challenges in the collection and other limiting factors [66,69]. Here, two types of biomass are considered:

- *Wet biomass*. This includes primary agricultural residues such as dry manure from poultry, sheep, goat manure, and wet manure from pits and cattle. Wet biomass serves as feedstock for the anaerobic digestion process. Fig. 2c visualizes the spatially-resolved technical wet biomass potentials taken from [66]. The aggregated wet biomass potential is about 170 Mt.
- *Dry biomass*. This includes agriculture and forestry residues such as wood chips and pellets. Dry biomass serves as feedstock for the gasification process. Fig. 2d visualizes the spatially-resolved technical dry biomass potentials taken from [66]. The aggregated dry biomass potential is about 370 TWh.

The wet and dry biomass prices are taken from [66]. Finally, the carbon intensities of natural gas, wet biomass, and dry biomass include fuel supply chain emissions and are taken from [26,27].

2.2. Hydrogen production

The available hydrogen production technologies are (i) steam methane reforming (SMR) from natural gas or biomethane, (ii) proton exchange membrane electrolysis from electricity, and (iii) biomass gasification. Excess electricity produced through the combustion of tail gases from SMR or gasification can be used to power electrolyzers, hydrogen conditioning, or carbon conditioning technologies. If the excess electricity is not consumed by another process, it has to be exported to the grid, as electricity transport between nodes is not included. Furthermore, SMR from natural gas or biomethane and biomass gasification can be coupled with CCS to reduce process emissions. When starting from biomass, a carbon removal is generated resulting in net-negative process emissions (Table 1). The techno-economic parameters of the available hydrogen production technologies are taken from [26,27,70–72].

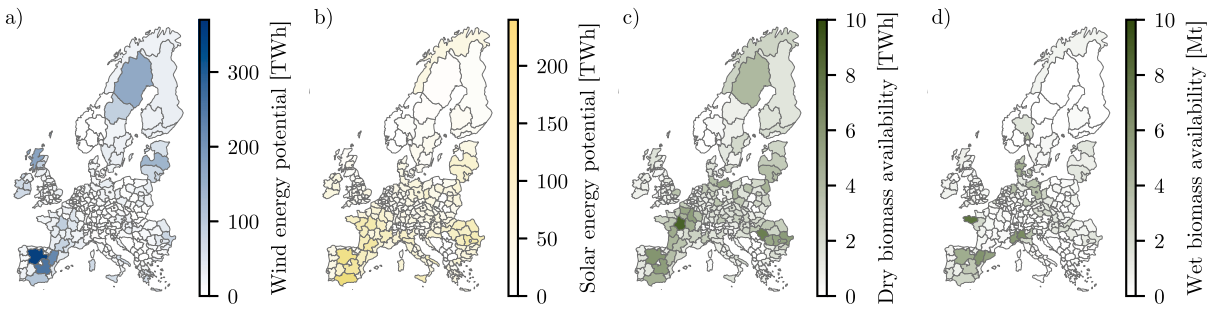

Fig. 2. Spatially-resolved technical potentials of renewable energy sources in Europe: (a) wind energy, (b) solar energy, (c) dry biomass, and (d) wet biomass [65,66]. Dry biomass includes woody residues from agriculture and forestry. Wet biomass includes agricultural primary residues such as manure.

2.3. Hydrogen transport

Several hydrogen transport options exist: ISO-tank containers (isotainers) loaded on trucks, trains, barges, and ships, and pipelines [23,73]. [74] investigate the trade-offs between the different transport options and identify transport volume and distance as the key drivers for the cost-optimal transport strategy.

In this work, hydrogen can be transported via isotainers loaded on trucks in its gaseous or liquid form. Hydrogen transport via pipeline is not considered because we focus on commercially available solutions that are readily deployable to decarbonize hydrogen supply chains in the near term. While pipelines are identified as the most cost-effective transport option over long distances and for larger volumes [74,75], they require high capital investment, long construction times, and complex regulatory backgrounds, which might prevent their deployment in the immediate future [76]. Similarly, while existing natural gas pipelines could be repurposed for transporting hydrogen and carbon, it is highly uncertain when and where the conditions for repurposing are fulfilled [76].

Hydrogen is produced at ambient temperature (25 °C) and pressures of 30 bar [23]. Even though the specific energy content of hydrogen is high (33 kWh/kg), the density of hydrogen at ambient temperature and pressures of 30 bar is low (2.4 kg/m^3) [77]. To reduce specific transport costs, higher energy densities are required. Therefore, hydrogen is typically transported as a compressed gas at ambient temperature and high pressures between 200-350 bar, or as a liquid (−253 °C, 1 bar) [77,78].

Hence, different transport modes require the installation of compression, liquefaction, and evaporation technologies. We model these technologies following [23,74]. The techno-economic parameters of the hydrogen transport and conditioning technologies are based on [23,70,77].

2.4. Hydrogen demand

Fig. 3 shows the 2020 (left), and projected 2035 (right) hydrogen demands for refineries, ammonia, methanol and other chemicals (e.g., polymers, and polyurethanes). The hydrogen demands are aggregated at a regional level, following the EU nomenclature of territorial units for statistics (NUTS) for level 2 (NUTS2) [61], and the locations and hydrogen demands of the ammonia production plants (pink circles), and the refineries (green circles) are visualized. While the hydrogen demand from ammonia (103 TWh), methanol production and other chemicals (36 TWh) is expected to remain constant until 2035 [5,79], the hydrogen demand from refineries is expected to decrease from 146 TWh to 70 TWh as the demand for fossil fuels reduces [16]. In 2020, 96% of the hydrogen was produced on-site via steam methane reforming from natural gas [7]. The existing SMR production capacities are taken from [80].

2.5. Carbon supply chain

A carbon supply chain is coupled with the HSC to account for the transport of the captured carbon to a designated carbon storage site. In this work, the Northern Lights project in Norway is considered as the designated carbon storage site [82] and is modeled following [83]. Several carbon transport options exist, including isotainers loaded on trucks and pipelines [70,75]. The installation of carbon pipelines is not considered, as we focus on commercially available solutions that can be deployed in the near term and do not face regulatory barriers or long construction times.

When considering transport on isotainers, carbon is typically transported as a liquid at 22 bar and −35 °C. Thus, carbon liquefication units must be installed [73]. The carbon liquefaction is modeled following [75,84]. The techno-economic input parameters of the carbon transport technologies are based on [70,75].

2.6. Biomass supply chain

Wet biomass. The collection and transport of wet biomass is challenging [85]. Considering the technical difficulties and economic constraints, maximum transport distances between 10–50 km are reported in literature [85,86]. Therefore, we assume that wet biomass cannot be transported and is only used where available.

Dry biomass. Dry biomass can be transported for longer distances via containers loaded on trucks or trailers pulled by tractors [69,85]. Here, we consider dry biomass transport via containers loaded on trucks. Dry biomass transport overcomes spatial constraints and enables on-site hydrogen production. The techno-economic parameters for dry biomass transport are taken from [85].

3. Formulation of the optimal design problem

The optimization problem is formulated as a linear program (LP) and includes continuous variables $\mathbf{x}$. In its general form, the LP is written as

$$\begin{aligned} \min_{\mathbf{x}} \quad & J = \mathbf{c}^{\mathrm{T}}\mathbf{x} \\ \text{s.t.} \quad & \mathbf{A}\mathbf{x} \leq \mathbf{b} \\ & \mathbf{x} \in \mathbb{R}^{\mathrm{N}} \end{aligned} \tag{1}$$

where J is the objective function, which is expressed as a linear combination of the continuous decision variables $\mathbf{x}$ and coefficient $\mathbf{c}$; matrix $\mathbf{A}$ represents the constraint matrix, vector $\mathbf{b}$ represents the known values of the constraints, and N represents the dimension of the continuous decision variables $\mathbf{x}$.

The optimization problem is implemented in the optimization framework ZEN-garden (Zero-emissions Energy Networks), developed at the Reliability and Risk Engineering Lab at ETH Zurich. ZEN-garden optimizes the design and operation of energy system models to investigate transition pathways toward decarbonization. The optimization problem is solved using the commercial solver Gurobi [87]. The following describes the input data, decision variables, constraints, and objective function of the optimization problem.

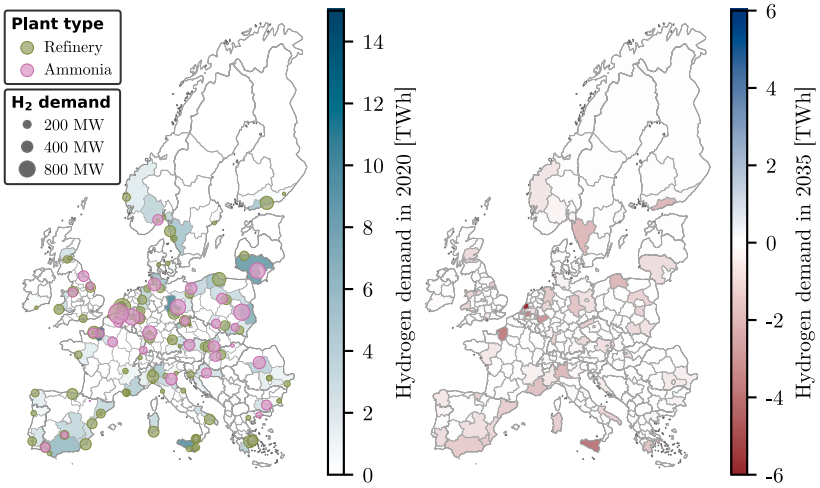

Fig. 3. Spatially resolved hydrogen demands for 2020 (left) [5,80], and expected increase (blue) and decrease (red) in hydrogen demand by 2035 (right) [16,79]. Hydrogen demand is aggregated at the NUTS2 level and indicated by the color bar. The locations and corresponding hydrogen demands of refineries (green circles) and ammonia production plants (pink circles) are visualized. Methanol production is typically co-located with refineries [81]. Therefore, the hydrogen demand of refineries here includes the hydrogen demand from methanol production.

3.1. Input data

The input data to the optimization problem are (i) the spatially-resolved hydrogen demands, the carrier prices, carbon intensities, and the availabilities of biomass, wind, and solar energy, (ii) the techno-economic parameters describing cost and performance of production, conditioning, and transport technologies, (iii) the existing hydrogen production capacities, (iv) the size and location of the available carbon storage sites, and (v) the target decarbonization pathways (Section 3.7). A yearly resolution is used to model the hydrogen demands, the carrier prices, the carbon intensity of the electricity grid, and the biomass availabilities. The remaining parameters are assumed constant. The supporting information [62] details the input data.

3.2. Decision variables

Two levels of spatial resolution are considered: regional (NUTS2) and national (NUTS0). Each region or country is represented by a node. At each node, hydrogen production, carbon capture, and conditioning technologies (i.e., conversion technologies) can be installed. Electricity and natural gas can be imported from the grids, excess electricity can be exported to the grid, and (if available) dry and wet biomass can be consumed. Edges connect the nodes. The distance between two nodes is approximated by their angular distance. At each edge, hydrogen, carbon, and dry biomass transport technologies can be installed.

The optimization problem determines the following decision variables:

- The capacity $S_{h,p,t}$ of technology h at position p and time t, with conversion technologies located at nodes and transport technologies located at edges,
- the carrier inputs $\underline{G}_{c,h,n,t}$, and the carrier outputs $\overline{G}_{c,h,n,t}$ of carrier c and conversion technology $h \in \mathcal{I}$ at node n and time t,
- the carrier flows $F_{c,h,e,t}$ of carrier c through transport technology $h \in \mathcal{J}$ along edge e and time t,
- the carrier imports $\underline{U}_{c,n,t}$ and exports $\overline{U}_{c,n,t}$ for carrier c at node n and time t.

3.3. Constraints

The constraints of the optimization problem are grouped into three categories: (i) mass balances, (ii) constraints modeling the behavior of the individual conversion and transport technologies, and (iii) carbon emission constraints.

3.3.1. Mass balances

The set of carriers C includes hydrogen, natural gas, electricity, dry biomass, wet biomass, and carbon. For each carrier $c \in C$, and for each node $n \in \mathcal{N}$, the mass balance at time $t \in \mathcal{T} = [0, T]$ can be expressed as:

$$\sum_{h\in\mathcal{I}}\left(\overline{G}_{c,h,n,t} - \underline{G}_{c,h,n,t}\right) + \sum_{h\in\mathcal{J}}\left(\sum_{e\in\underline{\mathcal{E}}_n} F_{c,h,e,t} - \sum_{e\in\overline{\mathcal{E}}_n}\left(F_{c,h,e,t} + F^{\mathrm{l}}_{c,h,e,t}\right)\right) + \overline{U}_{c,n,t} - \underline{U}_{c,n,t} - d_{c,n,t} = 0 \tag{2}$$

where $\underline{G}_{c,h,n,t}$ and $\overline{G}_{c,h,n,t}$ are the carrier input and output flows of conversion technology $h \in \mathcal{I}$ at node n and time t. $F_{c,h,e,t}$ and $F^{\mathrm{l}}_{c,h,e,t}$ represent the carrier flow, and the carrier flow loss of carrier c and transport technology $h \in \mathcal{J}$ at time t along edge e, where $\underline{\mathcal{E}}_n$ and $\overline{\mathcal{E}}_n$ represent the set of edges going in and out of node n, respectively. $\underline{U}_{c,n,t}$ is the import, $\overline{U}_{c,n,t}$ is the export, and $d_{c,n,t}$ is the demand of carrier c at node n and time t.

While the import of natural gas and grid electricity is not restricted, the import of wet and dry biomass is limited by their technical potential $a_{c,n,t}$ (Fig. 2c–d):

$$\underline{U}_{c,n,t} \le a_{c,n,t} \quad \forall c \in \{\text{dry biomass, wet biomass}\} \tag{3}$$

Furthermore, excess electricity, which is not used within the system, can be exported, i.e., $\overline{U}_{\text{electricity},n,t} \ge 0$. The remaining carriers cannot be exported, i.e. $\overline{U}_{c,n,t} = 0, \quad \forall c \in C \setminus \{\text{electricity}\}$.

3.3.2. Technology constraints

The capacity of technology h at position p and time t is described by $S_{h,p,t}$. Conversion technologies $h \in \mathcal{I}$ are located at nodes $p = n \in \mathcal{N}$ and transport technologies $h \in \mathcal{J}$ are located at edges $p = e \in \mathcal{E}$. In each time step, the capacity $S_{h,p,t}$ can be increased by $\Delta S_{h,p,t}$. The existing capacity is described by the parameter $s^{\mathrm{ex}}_{h,p,\bar{t}}$, where $\bar{t} \in [-l_h, 0]$. Hence, the capacity $S_{h,p,t}$ is defined as the sum of capacity increases $\Delta S_{h,p,t}$ and the existing capacity $s^{\mathrm{ex}}_{h,p,\bar{t}}$ with respect to the technology lifetime l_h:

$$S_{h,p,t} = \underbrace{\sum_{\bar{t}=\max(0,t-l_h+1)}^{t} \Delta S_{h,p,\bar{t}}}_{\text{Capacity increase}} + \underbrace{\sum_{\bar{t}=min(t-l_h+1,0)}^{0} s^{\mathrm{ex}}_{h,p,\bar{t}}}_{\text{Capacity of existing technologies}}, \tag{4}$$

The capacity $S_{h,p,t}$ and the capacity increase $\Delta S_{h,p,t}$ are limited by $s^{\max}_{h,p}$, and $\Delta s^{\max}_{h}$, respectively:

$$0 \le S_{h,p,t} \le s^{\max}_{h,p} \tag{5}$$

$$0 \leq \Delta S_{h,p,t} \leq \Delta s_h^{\max} \tag{6}$$

Conversion technology constraints. The performance of a conversion technology $h \in \mathcal{I}$ that converts input carriers $c \in \underline{C}_h$ into output carriers $c' \in \overline{C}_h$ is described by the conversion efficiency $\eta_{h,c,c'}$:

$$\overline{G}_{c',h,n,t} = \eta_{h,c,c'} \underline{G}_{c,h,n,t} \tag{7}$$

Each conversion technology $h \in \mathcal{I}$ has a single reference carrier $c_h^{\mathrm{r}} \in \overline{C}_h$. The capacity of conversion technology h provides an upper limit to the output flow of the reference carrier. For example, for electrolysis, the hydrogen output flow is limited by the installed electrolyzer capacity.

$$\overline{G}_{c_h^{\mathrm{r}},h,n,t} \leq S_{h,n,t} \tag{8}$$

The carbon storage is also modeled as a conversion technology that takes carbon and electricity as inputs and does not produce any output. The capacity of the carbon storage sites is limited by $s_{h,n}^{\max}$ and provides an upper limit to the carbon input flow.

Finally, existing SMR capacities can be retrofitted with a carbon capture unit to reduce process emissions. We model the retrofitting of the existing SMR capacities by coupling the reference carrier flows of the carbon capture unit (carbon, CO_2) and the existing SMRs (hydrogen, H_2), thereby limiting the carbon output of the carbon capture (CC) unit in relation to the hydrogen production of the existing SMR capacities:

$$\overline{G}_{\mathrm{CO_2,CC},n,t} \leq \eta_{\mathrm{CC,CO_2,H_2}} \overline{G}_{\mathrm{H_2,SMR},n,t} \tag{9}$$

where the parameter $\eta_{\mathrm{CC,CO_2,H_2}}$ is a conversion factor that describes how much carbon can be captured per unit of hydrogen produced.

Transport technology constraints. For each transport technology $h \in \mathcal{J}$, the installed capacity $S_{h,e,t}$ provides an upper limit to the carrier flow $F_{c,h,e,t}$:

$$F_{c,h,e,t} \leq S_{h,e,t} \tag{10}$$

Furthermore, the carrier flow $F_{c,h,e,t}$ is subject to losses. For each transport technology $h \in \mathcal{J}$ the losses ρ_h are modeled proportionally to the transport distance $\lambda_{h,e}$:

$$F_{c,h,e,t}^{\mathrm{l}} = \rho_h \lambda_{h,e} F_{c,h,e,t} \tag{11}$$

Energy requirements for conditioning. The conditioning technologies are modeled as conversion technologies that use electricity to bring carriers from the production conditions to the conditions required for transport. Both, hydrogen and carbon require conditioning. The electricity consumption required for conditioning is calculated following [23,77].

3.3.3. Carbon emission constraints

The total carbon emissions of the system must comply with the decarbonization target e_t (Section 3.7):

$$e_t \leq \sum_{n\in\mathcal{N}} \sum_{c\in\mathcal{C}} \epsilon_c \underline{U}_{c,n,t} + \sum_{n\in\mathcal{N}} \sum_{h\in\mathcal{I}} \epsilon_h \overline{G}_{c_h^{\mathrm{r}},h,n,t} + \sum_{e\in\mathcal{E}} \sum_{h\in\mathcal{J}} \sum_{c\in\mathcal{C}} \epsilon_h \lambda_{h,e} F_{c,h,e,t} \tag{12}$$

where ϵ_c describes the direct and indirect carbon emissions that arise with the import and consumption of carrier c. Furthermore, ϵ_h quantifies the direct and indirect carbon emissions that are not connected to the feedstock but arise when operating conversion technologies $h \in \mathcal{I}$ and transport technologies $h \in \mathcal{J}$, respectively.

3.4. Objective function

The optimization minimizes the total net present cost of the supply chain NPC. This includes the capital expenditures CAPEX_t and the operational expenditures OPEX_t. The net present value discounts the future cash flows via a constant discount rate of $r = 6\,\%$:

$$\mathrm{NPC} = \sum_{t\in\mathcal{T}} \frac{1}{(1+r)^t} \left(\mathrm{CAPEX}_t + \mathrm{OPEX}_t\right) \tag{13}$$

The capital expenditures, CAPEX_t, are computed by multiplying (1) the unit cost of the capital investment α_h with the capacity $S_{h,p,t}$ for each technology $h \in \mathcal{H}$ and (2) the unit cost of the capital investment per distance $\hat{\alpha}_h$ with the capacity $S_{h,e,t}$ and the transport distance $\lambda_{h,e}$ for each transport technology $h \in \mathcal{J}$:

$$\mathrm{CAPEX}_t = \sum_{p\in\mathcal{P}} \sum_{h\in\mathcal{H}} \alpha_h S_{h,p,t} + \sum_{e\in\mathcal{E}} \sum_{h\in\mathcal{J}} \hat{\alpha}_h \lambda_{h,e} S_{h,e,t} \tag{14}$$

The operational expenditures, OPEX_t, are computed as the sum of (1) the carrier cost, (2) the fixed operational expenditures, and (3) the variable operational expenditures for the conversion and transport technologies. The carrier cost is derived by multiplying the carrier unit cost u_c of each import carrier $c \in C^{\mathrm{imp}}$ with the carrier import $\underline{U}_{c,n,t}$. The fixed operational expenditures are calculated by multiplying the fixed operational unit cost γ_h of each technology $h \in \mathcal{H}$ with the installed capacity $S_{h,p,t}$, and the fixed operational unit cost per distance $\hat{\gamma}_h$ of each transport technology $h \in \mathcal{J}$ with the installed capacity $S_{h,p,t}$ and the transport distance $\lambda_{h,e}$. Finally, the variable operational expenditures for each conversion technology $h \in \mathcal{I}$ are calculated by multiplying the operational unit cost β_h with the reference output flow $\overline{G}_{c_h^{\mathrm{r}},h,n,t}$; and for each transport technology $h \in \mathcal{J}$ by multiplying the operational unit cost β_h and the unit cost per distance $\hat{\beta}_h$ with the carrier flow $F_{c,h,e,t}$ and the transport distance $\lambda_{h,e}$:

$$\begin{aligned}\mathrm{OPEX}_t = &\sum_{n\in\mathcal{N}} \sum_{c\in C^{\mathrm{imp}}} u_c \underline{U}_{c,n,t} + \sum_{p\in\mathcal{P}} \sum_{h\in\mathcal{H}} \gamma_h S_{h,n,t} + \sum_{e\in\mathcal{E}} \sum_{h\in\mathcal{J}} \hat{\gamma}_h \lambda_{h,e} S_{h,e,t} \\ &+ \sum_{n\in\mathcal{N}} \sum_{h\in\mathcal{I}} \beta_h \overline{G}_{c_h^{\mathrm{r}},h,n,t} + \sum_{e\in\mathcal{E}} \sum_{h\in\mathcal{J}} \sum_{c\in\mathcal{C}} \left(\beta_h + \hat{\beta}_h \lambda_{h,e}\right) F_{c,h,e,t}\end{aligned} \tag{15}$$

3.5. Levelized cost of hydrogen

Here, we adopt an approach similar to the levelized cost of energy (LCOE) to assess the levelized cost of hydrogen (LCOH). The LCOE is an economic concept commonly used to compare alternative energy production technologies. The LCOE is defined as the net present cost divided by the net present energy production, which is obtained by discounting the present energy production over future years [88,89]. Here, we use the LCOH to compare different hydrogen production technologies and HSC designs. The LCOH is derived as the total net present cost of the supply chain NPC divided by the total net present hydrogen production O:

$$\mathrm{LCOH} = \frac{\mathrm{NPC}}{O} \tag{16}$$

The net present hydrogen production O is computed by discounting the present hydrogen production over the future years:

$$O = \sum_{t\in\mathcal{T}} \frac{1}{(1+r)^t} \sum_{h\in I} \sum_{n\in N} \overline{G}_{\mathrm{H_2},h,n,t}, \tag{17}$$

where $\overline{G}_{\mathrm{H_2},h,n,t}$ describes the present hydrogen (H_2) production by conversion technology $h \in \mathcal{I}$ at node n and time t.

3.6. Quantifying the impact of spatial resolution

To investigate the impact of spatial resolution on the optimal supply chain design, the optimization is solved for two levels of spatial resolution, regional (NUTS2) and national (NUTS0). Furthermore, the impact of spatial resolution on the LCOH is quantified. To this end, the regional optimization (NUTS2) is augmented by an additional constraint, which limits the capacity of the hydrogen production technologies that are installed at the nodes n within a country m in the regional model (NUTS2) to the capacity of the hydrogen production technologies that is installed in country m in the national model (NUTS0):

$$\sum_{n\in\mathcal{N}_m^{\mathrm{C}}} S_{h,n,t} \leq s_{h,m,t}^{\lim} \tag{18}$$

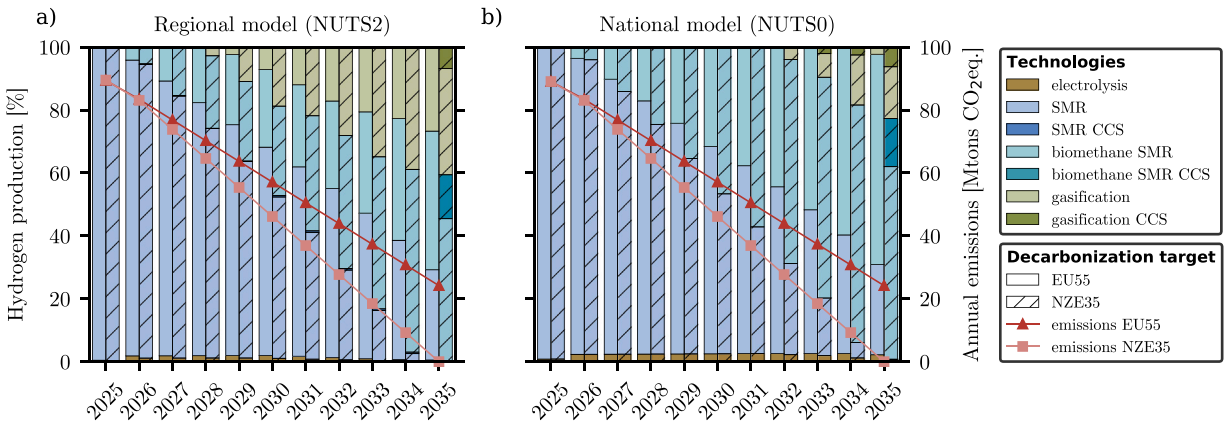

Fig. 4. Cost-optimal hydrogen production technology mix (bars, left-hand side y-axis) and cumulative carbon emissions (lines, right-hand side y-axis) for each year of the 2025–2035 time horizon. Two scenarios are presented: the EU55 target (left bar, dark red line) and the NZE35 target (right bar with hatches, light red line). The set of hydrogen production technologies includes water-electrolysis from electricity, steam methane reforming (SMR) from natural gas, biomethane reforming from wet biomass, and biomass gasification from dry biomass. Hydrogen production technologies using carbonaceous feedstock (natural gas, biomass) can be coupled with carbon capture and storage (CCS).

$S_{h,n,t}$ represents the capacity of hydrogen production technology $h \in \mathcal{I}$ at node n and time t, $\mathcal{N}_m^{\mathrm{C}}$ represents the set of nodes within country m, and $s_{h,m,t}^{\mathrm{lim}}$ describes the capacity of hydrogen production technology $h \in \mathcal{I}$ that was installed by the national model in country m at time t. Hence, this additional constraint forces the regional model's design decisions (NUTS2) to follow the national model's design recommendations (NUTS0) and results in the model NUTS0-2.

In addition, a slack variable e_t^{o} is added to the carbon emissions constraint to relax the carbon emissions limit e_t and ensure the feasibility of the NUTS0-2 optimization:

$$e_t - e_t^{\mathrm{o}} \leq \sum_{n\in\mathcal{N}}\sum_{c\in\mathcal{C}} \epsilon_c \underline{U}_{c,n,t} + \sum_{n\in\mathcal{N}}\sum_{h\in\mathcal{I}} \epsilon_h \overline{G}_{c_h^{\mathrm{r}},h,n,t} + \sum_{e\in\mathcal{E}}\sum_{h\in\mathcal{J}}\sum_{c\in\mathcal{C}} \epsilon_h \lambda_{h,e} F_{c,h,e,t} \quad (19)$$

The slack variable e_t^{o} can be interpreted as the carbon emissions overshoot at time t. The slack variable is added to the objective function and multiplied by the carbon emission overshoot price μ^{o}, which is a value sufficiently large to ensure that the overshoot of the emissions limit is selected as a last resort (an overshoot price of 9000 €/tCO_2 is selected here, which is high enough but does not result in numerical issues):

$$\mathrm{NPC} = \sum_{t\in\mathcal{T}} \frac{1}{(1+r)^t} \left(\mathrm{CAPEX}_t + \mathrm{OPEX}_t + \mu^{\mathrm{o}} e_t^{\mathrm{o}}\right) \quad (20)$$

3.7. Decarbonization pathways

The optimal design of the HSC is performed for different decarbonization targets to assess their impact on the optimal design and rollout of HSCs.

Ten decarbonization targets are investigated, ranging from no decarbonization (0 % target) to an ambitious target of net-zero supply chain emissions by 2035 (100 % target, NZE35). For each decarbonization target, a linear pathway is assumed, where the system emissions decrease linearly from the initial value in the first year (2025) to the target value in the last year (2035).

In addition, we investigate the policy-based EU Fit for 55 target (EU55), which calls for a 55 % reduction of carbon emissions by 2030 with respect to 1990 and aims for carbon neutrality by 2050 [90]. Emissions from industry have decreased by 29% with respect to 1990 [91]. Hence, carbon emissions need to be reduced by an additional 26% by 2030 to fulfill the EU55 target. This corresponds to a 37% reduction with respect to the emissions reported in 2021. Therefore, we implement the EU55 scenario such that the supply chain emissions decrease by 37% from 2025 to 2030 and continue to decrease linearly from 2030 to 2035.

4. Optimal design of low-carbon hydrogen supply chains with high spatial resolution

We investigate the optimal rollout of low-carbon hydrogen supply chains to decarbonize the existing European hydrogen demands from refineries, ammonia production, methanol production, and other chemicals by 2035. We take a near-term perspective (2025–2035) and study the impact of spatial resolution on the optimal design of low-carbon HSCs by comparing two levels of spatial resolution, namely regional (NUTS2) and national (NUTS0). The analysis focuses on four aspects of the supply chains: First, Section 4.1 illustrates the optimal transition from carbonaceous hydrogen production to low-carbon hydrogen production from 2025–2035 for the EU55 and the NZE35 decarbonization targets. Second, Section 4.2 compares the optimal investment strategies for different decarbonization targets, ranging from no decarbonization (0%) to full decarbonization (100%, NZE35 target). Third, Section 4.3 studies the optimal network designs of the hydrogen, carbon, and biomass supply chains in the NZE35 target, where the impact of spatial resolution is most pronounced. Fourth, Section 4.4 quantifies the impact of spatial resolution in terms of cost by comparing the levelized cost of hydrogen (LCOH) across the different HSC designs.

4.1. Cost-optimal hydrogen production technology mix

Fig. 4a shows the evolution of the optimal technology mix and the cumulative carbon emissions from 2025 to 2035 for the EU55 and the NZE35 target in the regional model (NUTS2).

EU55. In 2025, hydrogen production is dominated by SMR from natural gas. Existing SMR capacities are used to produce hydrogen on-site, which is in line with the status quo. In addition, excess electricity from the SMR processes is used to power a small share of electrolyzers (about 2 %). With increasing decarbonization targets, biomethane continuously replaces natural gas to reduce process emissions (44% by 2035). In addition, starting in 2029, biomass gasification is deployed (27% by 2035). The two measures are sufficient to realize the EU55 target.

NZE35. The realization of the NZE35 target requires additional measures. By 2035, biomethane reforming and biomass gasification have completely replaced SMR from natural gas. In addition, about 17 % of biomass gasification and about 24% of biomethane reforming is coupled with CCS to generate the carbon removal required to achieve net-zero emissions by 2035. Electrolysis plays a minor role, and shares remain below 2% over the entire time horizon.

Fig. 4b shows the evolution of the optimal technology mix and the cumulative carbon emissions from 2025 to 2035 in the national model

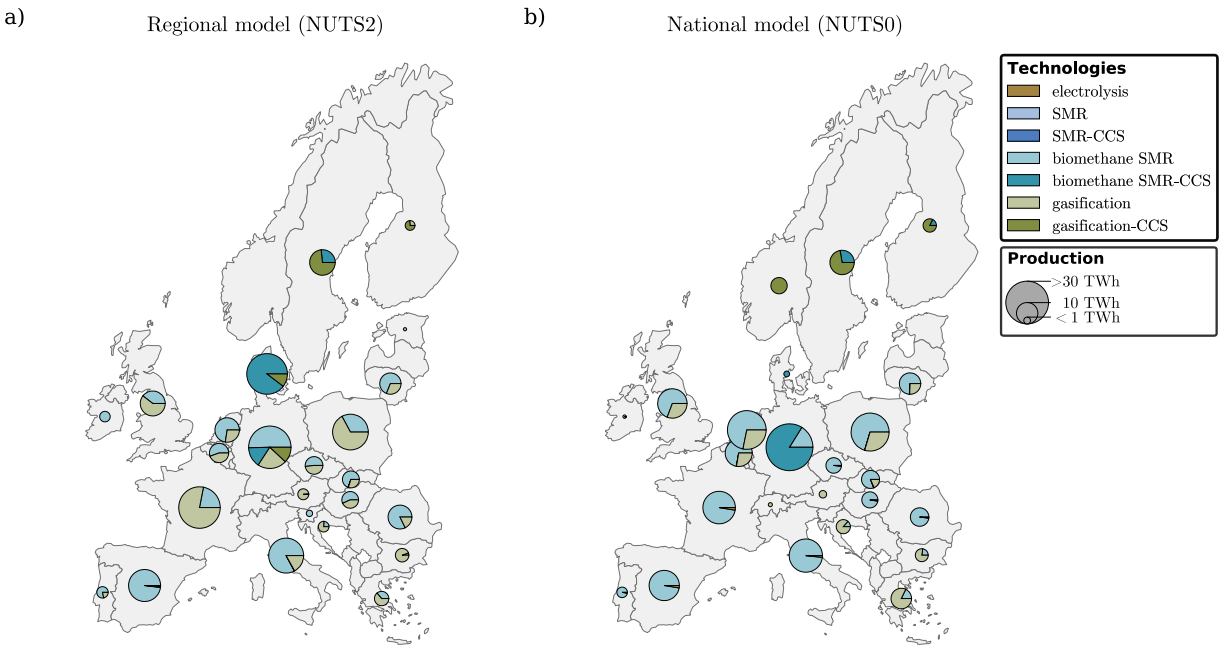

Fig. 5. Cost-optimal hydrogen production volumes and technology mix for net-zero hydrogen supply chains in the regional (NUTS2) (a) and national (NUTS0) (b) model.

(NUTS0). Both models achieve the EU55 target by replacing natural gas with biomethane and deploying biomass gasification. Compared to the regional model (NUTS2), the national model deploys much higher shares of biomethane reforming (+23 %) and only small shares of biomass gasification (−24 %).

The realization of the NZE35 target requires investments in CCS, and both models couple about 21 % of their total hydrogen production with CCS. Compared to the regional model, the national model deploys larger shares of biomethane reforming (+17%) and installs less biomass gasification (−18%).

Despite the differences in the transition, which are more pronounced for the stricter emission target of the NZE35 scenario, some general conclusions can be drawn: Biomethane reforming is identified as the most cost-effective low-carbon hydrogen production technology. Replacing natural gas with biomethane reduces process emissions significantly, while the existing SMR capacities can be refurbished. Besides installing anaerobic digesters to produce biomethane, no additional investments are required.

However, biomethane reforming is associated with higher process emissions than biomass gasification (+16 gCO_2/kWh) and electrolysis from wind energy (+19 gCO_2/kWh). Hence, increasing decarbonization targets require the installation of biomass gasification or electrolysis and the coupling with CCS.

Fig. 5 highlights the differences for net-zero HSCs by comparing the optimal production volumes and technology mix for each country in (a) the regional model (NUTS2) and (b) the national model (NUTS0). The additional information regarding the regional hydrogen demands, the resource availabilities, and a better representation of the transport distances in the regional model lead to substantially different HSC designs. The differences are most pronounced for Denmark (+25 TWh increase in production volume from NUTS0 to NUTS2), the Netherlands (−14 TWh), France (+10 TWh), and Germany (−6 TWh). While the technology mix in the Netherlands and Denmark stays similar, it changes significantly for Germany and France. Both, the regional and the national model rely primarily on existing SMR capacities, where natural gas feedstocks are replaced by biomethane. However, the wet biomass potentials and the existing SMR capacities are not always aligned at the regional level. To resolve this mismatch, the regional model either (i) imports hydrogen from neighboring regions (e.g., Spain or Italy), or (ii) switches to alternative low-carbon hydrogen production pathways (e.g., Germany, France) to meet its hydrogen demands. Section 4.3 provides a more detailed discussion of the hydrogen, carbon, and biomass transport infrastructures visualized in Fig. 7.

4.2. Investment strategies to decarbonize hydrogen production

To unveil the rationale behind the optimal technology mix, we investigate the optimal investment strategies in the regional (a) and national model (b) for each decarbonization target as a function of time (Fig. 6). The decarbonization targets range from no decarbonization in 2035 (0 %) to full decarbonization in 2035 (100 %, NZE35). The red markers indicate the EU55 (dark red) and NZE35 (light red) targets.

For each decarbonization target, the optimal investment strategies indicate during which time-frame technologies are deployed. If more than one technology is deployed simultaneously, technology areas overlap. Indeed, the optimal investment strategy for the EU55 target in the regional model includes SMR from natural gas, biomethane reforming, and biomass gasification. In 2025, only SMR is deployed. Starting from 2026, biomethane reforming and SMR are deployed, and starting from 2030, biomass gasification is added to the technology mix as indicated by the overlapping areas in Fig. 6a.

A few considerations can be made for the individual hydrogen production technologies:

- *Biomethane reforming*. Replacing natural gas with biomethane is an effective measure that achieves decarbonization targets of up to 30% in the regional model and up to 65% in the national model.
- *Biomass gasification*. Biomass gasification is deployed to realize decarbonization targets above 30% in the regional, and 65% in the national model. With increasing decarbonization targets, the share of biomass gasification increases. In the regional model, up to 34% of the hydrogen demand is met with biomass gasification to achieve the NZE35 target, 17% more than in the national model.
- *Biomass-based hydrogen production coupled with CCS*. Independently of the level of spatial resolution, the realization of decarbonization targets above 92 % requires the coupling of biomass-based hydrogen production with CCS to offset carbon emissions that arise in connection with hydrogen production and transport,

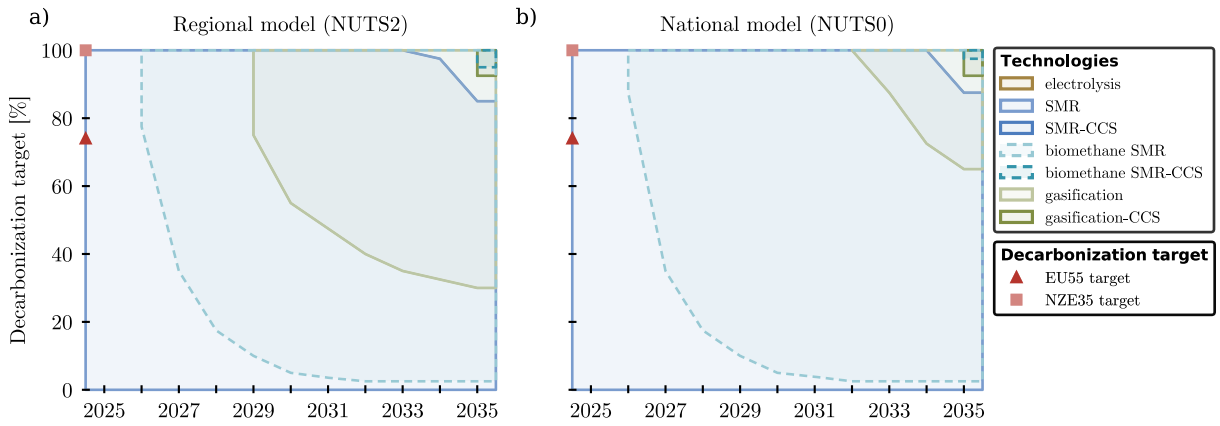

Fig. 6. Optimal investment strategies in the regional (a) and national model (b) as a function of time (2025–2035 time horizon) and decarbonization targets in 2035. The decarbonization targets range from no decarbonization target (0 %) to full decarbonization (100 %) by 2035. Technology shares below 3 % are not shown for simplicity. The red markers indicate the EU55 (dark red) and NZE35 (light red) targets.

and carbon and dry biomass transport. To achieve the NZE35 target, both models couple about 21% of their biomass-based hydrogen production with CCS. Biomass gasification coupled with CCS is deployed first in both models, starting with decarbonization targets above 92%. Biomethane reforming coupled with CCS follows, starting with decarbonization targets of 95% in the regional model, and 97% national model.

- *Electrolysis*. Electrolysis does not exceed the 3 % share and, thus, does not become cost-competitive on a large scale in both, the regional and the national model.

A technology ranking can be derived based on Fig. 6. Investments in biomethane reforming are followed by investments in biomass gasification, biomass gasification coupled with CCS, and finally, biomethane reforming coupled with CCS. Electrolysis plays a minor role and is only deployed at small scales. The major difference between the investment strategies of the regional and national model is the investment in biomass gasification: The regional model deploys larger shares of biomass gasification (>3 %) as early as 2029 compared to 2032 in the national model; and for lower decarbonization targets (30% in regional model vs. 65% in national model).

The higher spatial resolution of the regional model allows for a more accurate representation of the heterogeneous availability of renewable resources and regional hydrogen demands. With increasing decarbonization targets, as renewable resources successively replace fossil feedstocks, the differences between the regional and national models increase. The differences are most pronounced for fully decarbonized HSCs.

4.3. Net-zero hydrogen, carbon, and biomass supply chains

Fig. 7 compares the cost-optimal (a) hydrogen, (b) carbon, and (c) dry biomass supply chain designs for the NZE35 scenario in 2035 for the regional and national model. For the sake of comparison, the regional model results are aggregated at the national level (the regionally-resolved maps are reported in Section S4 [62]).

(a) Hydrogen supply chain. Fig. 7a shows the cost-optimal hydrogen transport infrastructure and production volume in 2035 for the regional (right) and national (middle) model and highlights their differences (left). In the regional model, about 55% of the hydrogen demand is satisfied through local production. To balance hydrogen production and demand, the regional model builds a European-wide hydrogen transport infrastructure, where, in particular, the northwest of Germany, Belgium, and the Netherlands are well connected (Figure S6 [62]).

Unlike the regional model, the national model does not build a European-wide hydrogen transport infrastructure. Countries with sufficient renewable resource potentials, such as France and Spain, are not connected with hydrogen transport infrastructure (Fig. 7a, middle). In fact, the national model satisfies 96% of the hydrogen demands locally. Countries where the resulting dry biomass consumption exceeds their availability (e.g., the Netherlands), import dry biomass from neighbors (Fig. 7c).

(b) Carbon supply chain. Fig. 7b shows the cost-optimal carbon transport infrastructure and capture volumes. Through the carbon supply chain, carbon is captured at the hydrogen production sites, conditioned, and transported to the underground storage site in Norway [82]. Both, the regional and the national model connect central and northern European countries with the storage location in Norway. About 11 Mt of carbon are captured in the regional model, and about 13 Mt in the national model, to offset emissions that arise from hydrogen production, and hydrogen, carbon, and dry biomass transport. To this end, the regional model installs carbon capture units in northern Germany, Denmark, Sweden, and Finland, whereas the national model places additional capture units in Norway. While the carbon supply chain network in the regional model covers about twice the distance than in the national model, the resulting average weighted transport distances are comparable (875 km in the regional model and 756 km in the national model). However, the resulting weighted average transport distances are significantly higher than the 300 km that the IPCC considers economically reasonable [92]. Nevertheless, so far, the underground carbon storage site in Norway is the only operational carbon storage site in Europe that can kick-start the development and deployment of a European carbon transport infrastructure backbone.

(c) Biomass supply chain. Fig. 7c shows the cost-optimal transport infrastructure and consumption of dry biomass. In the regional model, large amounts of dry biomass are consumed in France (34 TWh), Poland (22 TWh), and Germany (16 TWh), utilizing between 30% and 55% of their available dry biomass. Other countries, such as the Netherlands or Hungary exceed their local dry biomass availability and have to rely on dry biomass imports from neighboring countries. In the national model, Poland, Sweden, and the Netherlands are the largest dry biomass consumers with about 11 TWh. France exports about 23% (15 TWh) of its dry biomass, distributing it between the UK, the Netherlands, Germany, and Switzerland, where dry-biomass is between 20-40% more expensive.

Fig. 8 shows the cost-optimal consumption of wet biomass, which cannot be transported. Both, the regional and the national model rely heavily on wet biomass in their decarbonization strategies. In the national model, about 93 Mt wet biomass is consumed, corresponding to 55% of the European wet biomass potential. The largest consumer is Germany with about 20 Mt. Conversely, wet biomass consumption is about 20% lower in the regional model. The largest changes are observed in Germany, where consumption reduces by about 50% (10 Mt),

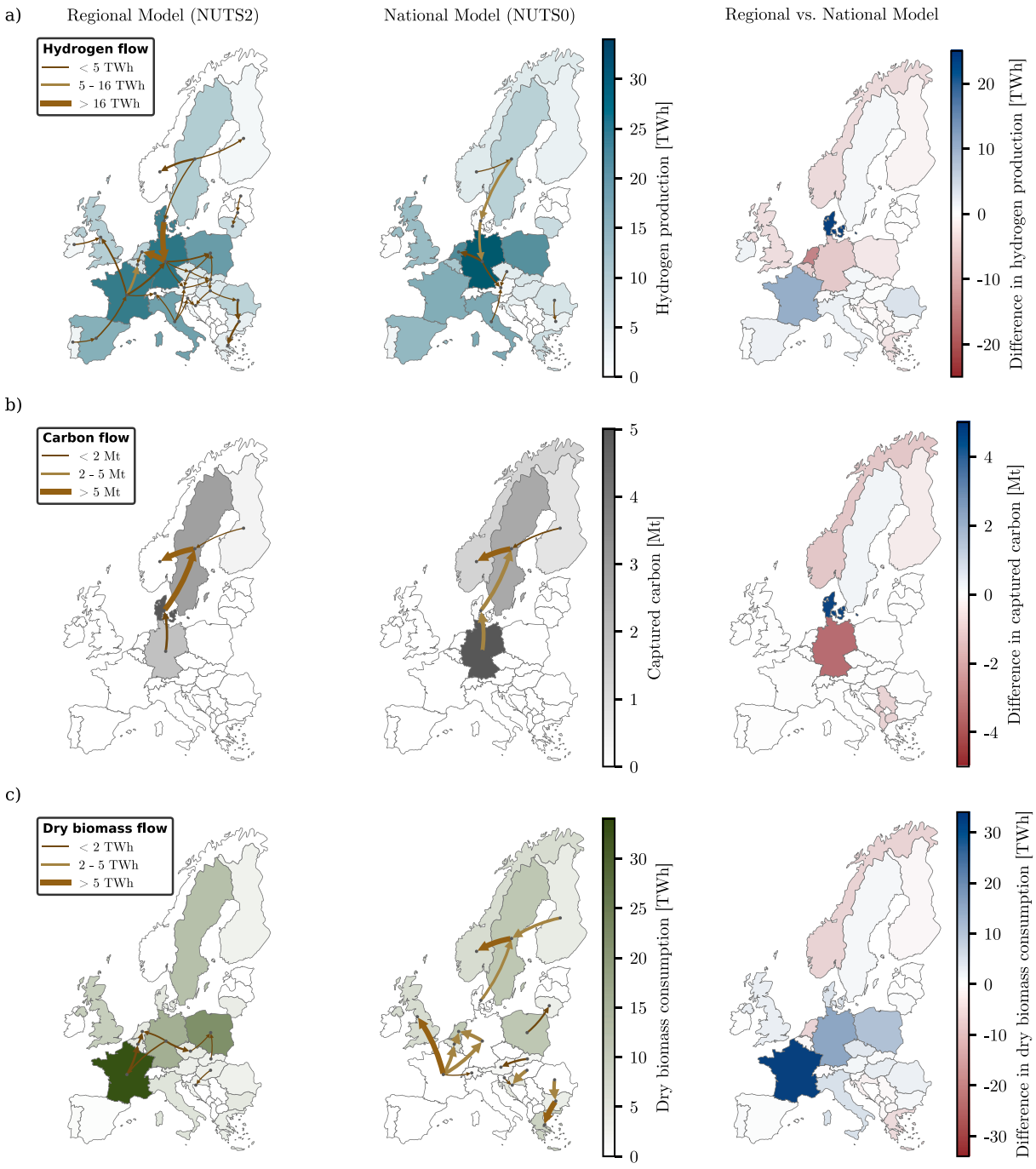

Fig. 7. Cost-optimal design of (a) hydrogen, (b) carbon, and (c) dry biomass supply chains in the regional (left) vs. national (middle) model in 2035 for the NZE35 scenario. The figures to the right highlight the differences between the regional and the national model.

and in France, the Netherlands, and Poland, where consumption reduces by about 60% (between 5–6 Mt).

The reduced wet biomass consumption in the regional model results from the misalignment of the regional wet-biomass availability and the existing hydrogen production capacities and demands. Instead, the regional model (i) shifts hydrogen production to neighboring regions and installs hydrogen transport technologies to decouple hydrogen production and consumption, or (ii) invests in alternative low-carbon hydrogen technologies, such as biomass gasification (Fig. 5). Unlike the regional model, the national model cannot capture the transport requirements on a sub-national level. As a result, the national model underestimates the cost and emissions that arise in connection with hydrogen, carbon, and biomass transport (Section 4.4), resulting in different design recommendations and infrastructure layouts (Figs. 5, 7 and 8). For instance, the national model installs large carbon capture capacities in Germany (5.2 Mt), as well as in Sweden (2.5 Mt) and Norway (1.3 Mt). By capturing carbon near the carbon storage site in Norway and Sweden, the cost and emissions arising from carbon transport are reduced. At the same time, the cost and emissions that arise in connection with hydrogen transport increase. In the regional model, no carbon capture capacities are used in Norway in 2035. Furthermore, the regional model reduces the carbon capture capacity in Germany by 65%, and moves hydrogen production capacities and carbon capture units to regions in Denmark (5 Mt), which are closer to the carbon storage site in Norway, and the hydrogen demands in northern Germany and the Netherlands. Although the regional model

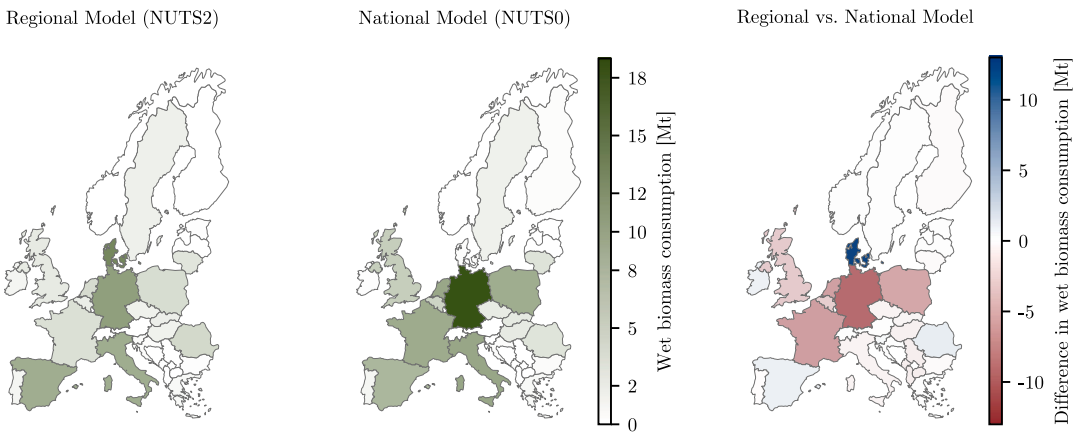

Fig. 8. Wet biomass consumption in the regional (left) vs. national (middle) model in 2035 for the NZE35 scenario. The differences between the regional and the national model are highlighted on the right.

offers a more accurate representation of the transport requirements, approximating the transport distances as the angular distances between the centroids of two regions might still lead to an underestimation of the transport distances for hydrogen, carbon, and dry biomass.

4.4. Impact of decarbonization targets and spatial resolution on levelized cost of hydrogen

Fig. 9 shows the cost breakdown of the levelized cost of hydrogen (LCOH) for the ten decarbonization targets, ranging from no decarbonization (0%) to full decarbonization (100%, NZE35). Here, the LCOH is used as a metric to aggregate cost over time and compare the different HSCs designs (Section 3.5). The LCOH is shown for the national model (NUTS0, left bar), the regional model (NUTS2, middle bar, hatches), and the regional model, constrained by the results of the national model (NUTS0-2, right bar, hatches, Section 3.6). Three regions are identified in relation to the decarbonization targets:

- *Negligible cost increase*. Decarbonization targets smaller or equal to 30 % can be realized with minimum cost increase (below 2%) compared to no decarbonization (0%). In this range, the LCOH of the regional and national models are comparable (<1% difference). Hydrogen is largely produced on-site from natural gas, and anaerobic digesters are installed to produce biomethane and replace natural gas as a feedstock in the steam methane reforming process. With increasing decarbonization targets, the anaerobic digestion capacities are expanded such that the decarbonization targets are met.
- *Moderate cost increase*. For decarbonization targets ranging from 40–70%, a steady cost increase of about 3% between the decarbonization targets is observed in the regional model. The differences between the regional and national models become more pronounced, with the LCOH in the regional model being up to 7% higher than in the national model. Natural gas is increasingly replaced by biomethane, and a hydrogen transport infrastructure is built to transport hydrogen from the production sites, where wet biomass is available, to consumption sites. In addition, the regional model increases investments in biomass gasification.
- *Steep cost increase*. For decarbonization targets above 70 %, a steep cost increase is observed in the regional model (up to 7% increase between decarbonization targets). Compared to the national model, the LCOH of the regional model is up to 18% higher. The main cost drivers are investments in hydrogen, carbon, and dry biomass transport infrastructure. In the national model, hydrogen demands and resources are spatially aggregated, neglecting domestic transport requirements. As a result, transport volumes and distances are underestimated. In particular, the conditioning step makes hydrogen and carbon transport costly. Hence, underestimating transport volumes reduces the conditioning requirements and leads to lower LCOH (Sections 4.1 and 4.3).

Furthermore, the impact of spatial resolution on the LCOH is quantified by solving the regional model following the design recommendations of the national model (Fig. 9, NUTS0-2). For small decarbonization targets in the range of 0-30%, the cost increase is negligible (less than 1% increase of LCOH from NUTS2 to NUTS0-2). For decarbonization targets ranging from 30–50% the LCOH increases up to 8%. However, for decarbonization targets above 50%, the LCOH increases up to 31%. The reasons for this large cost increase are, first and foremost, the carbon removal cost and the increasing hydrogen, carbon, and dry biomass transport costs.

In fact, without additional carbon removal, decarbonization targets above 50% cannot be realized when following the design recommendations of the national model. To achieve the NZE35 target, 50 Mt of carbon emissions have to be removed from the atmosphere between 2030 and 2035. Assuming carbon removal costs of 1300 €/t [93], this increases the total system cost by 66 M€, and results in a 29% (19 €/MWh) increase of the LCOH with respect to the optimal solution (NUTS2). However, considering current carbon prices, which are around 81 €/t (2022) [94], the additional cost to offset the carbon emissions would be about 4.1 million euro (M€). Compared to the hydrogen production cost and the hydrogen and carbon transport cost, the resulting increase in the total system cost is small and would not affect the LCOH significantly (1.2 €/MWh increase compared to the optimal solution in the regional model (NUTS2)).

Finally, a comparison with literature estimates from [21,32,95,96] shows that the LCOH for hydrogen produced from natural gas (1.5 €/kg vs. 0.66–1.33 €/kg), wet biomass (2.12 €/kg vs. 1.32 - 2.68 €/kg), dry biomass (3 €/kg vs. 1.8–3.22 €/kg), and renewable electricity (4.2 €/kg vs. 2.98–15.45 €/kg) are within the ranges reported in literature (Table 1 and Section S3 [62]).

5. Discussion

In the following, we discuss and contextualize our findings by comparing our results to related literature. In particular, the role of electrolyzers (Section 5.1) and the role of hydrogen and carbon transport infrastructure (Section 5.2) is discussed. Section 5.3 discusses the limitations of central model assumptions.

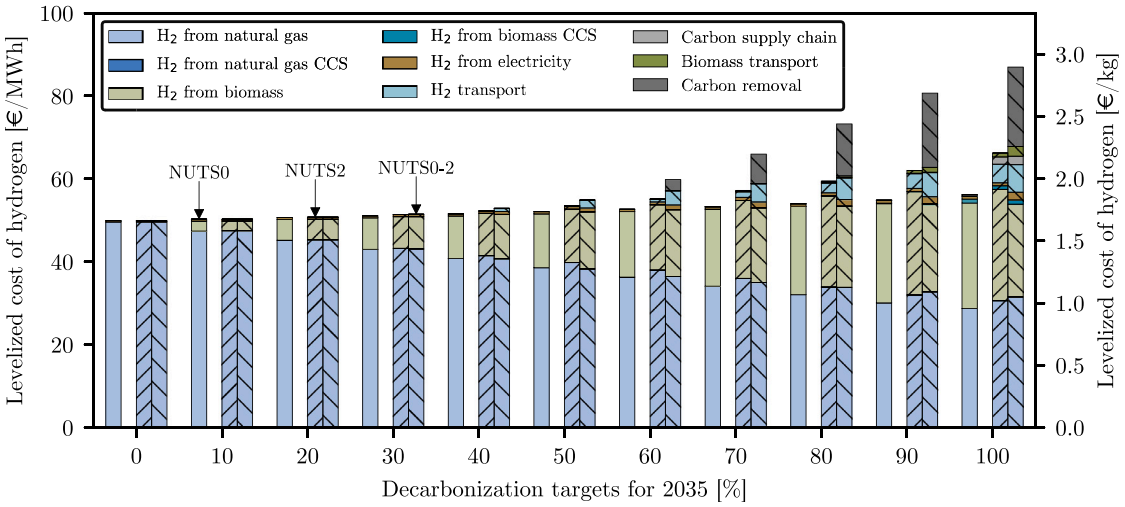

Fig. 9. Cost breakdown of the levelized cost of hydrogen (LCOH) as a function of ten decarbonization targets in 2035, ranging from no decarbonization (0 %) to full decarbonization (100 %, NZE35). The LCOH are presented for the national model (NUTS0, first bar, no hatches), the regional model (NUTS2, second bar, hatches), and the regional model, optimized following the design recommendations from the national model (NUTS0-2, third bar, hatches).

5.1. The role of electrolyzers in enabling the transition to low-carbon hydrogen

Electrolyzers are often viewed as a key technology for producing low-carbon hydrogen and enabling the energy transition across sectors [97,98]. To reduce the dependency on natural gas imports and improve security of supply while achieving the climate targets set for 2030 and 2050, the EU set the ambitious target of producing 10 Mt of low-carbon hydrogen by 2030 [99]. To this end, the EU envisions a scale-up of the existing electrolyzer capacities from 1.75 GW_{H_2} (2022) to 90–100 GW_{H_2} (2030) [12,99]. However, despite the strong momentum surrounding hydrogen, the ramp-up of low-carbon hydrogen production capacities remains slow, and the production of low-carbon hydrogen is expected to stay small throughout 2030 (less than 1% of final energy demand in Europe) [100]. The high upfront investment costs and the considerable uncertainty surrounding future investment costs delay investments, with risk-averse investors waiting until costs drop [101,102]. Continuous insufficient investments in low-carbon hydrogen production capacities will delay the development of low-carbon HSCs further, and thus, the three-sided "chicken-and-egg problem" pertains [15,100].

This work shows that biomass-based hydrogen production is more cost-efficient than water-electrolysis. Even when considering significantly lower investment costs (−25%) and increased efficiencies (+4%), electrolyzers do not become cost-competitive, and their contribution to the hydrogen production remains below 5% (Figure S11 [62]). These findings persist, even when considering increased energy commodity prices ([+12%, +38%], Figure S10 [62]) or a reduced discount rate from 6% to 2% (Figure S12 [62]). These findings are also in line with previous literature: For instance, [103] investigate hydrogen production technology shares for biomass- and electricity-based hydrogen production technologies and show that electrolyzers do not become cost-competitive with biomass gasification before 2035. Similarly, [104] investigate the cost-competitiveness of electrolytic hydrogen production and SMR-CCS. The authors show that electrolyzers are not expected to become cost-competitive before 2035 even in the most optimistic case. Therefore, biomass-based hydrogen production could provide a complementary solution to renewable-electricity-based hydrogen production, incentivizing investments in low-carbon hydrogen supply in the near term.

5.2. Hydrogen transport vs. on-site production

Our analysis shows that hydrogen production is not necessarily co-located with consumption sites. In contrast, a hydrogen network might help reduce costs towards net-zero hydrogen supply chains. Other studies have investigated the role of hydrogen supply chains. Similar to our work, [18,34] follow an optimization-based approach. [18] take a single-year perspective and investigate the role of HSCs in a fully decarbonized, sector-coupled energy system, whereas [34] take a multi-year perspective and investigate different transition pathways for a sector-coupled energy system. In both cases, a hydrogen transport infrastructure is found to reduce system costs across scenarios.

[34] design the hydrogen transport infrastructure with national resolution (NUTS0), and thus, do not capture intra-regional bottlenecks, possibly underestimating hydrogen transport requirements. In contrast, [16,18,105] design the HSC at the regional level. While [18,105] go beyond the industries investigated in this work, we identify a similar need for transport infrastructure in Spain, south France, north-west Germany, Belgium, and the Netherlands by 2030. Between 2030 and 2035, the transport infrastructure is expanded to comply with net-zero emissions in the NZE35 scenario. For net-zero supply chains, we identify a need for hydrogen transport infrastructure in north-west Germany, Belgium, the Netherlands, Italy, Spain, Romania, Bulgaria, and Greece similar to [18,105]. Moreover, [16] also assess the cost-effectiveness of hydrogen transport infrastructure to decarbonize hard-to-abate industries and include hydrogen demands from refineries, ammonia production, methanol production, steel production, and chemical plastics recycling. Although [16] do not follow an optimization-based approach, similar clusters are identified: (i) Belgium, The Netherlands, and north-west Germany, (ii) Poland and Lithuania, and (iii) Romania, Bulgaria and Greece.

While hydrogen transport via trucks is more expensive, especially compared to pipelines, we show that it is cost-efficient to install hydrogen transport infrastructure. Deploying ready-to-use transport technologies, such as trucks, can help to scale up transport infrastructure in the near term and establish transport routes until the pipeline networks envisioned by [18,105] become available.

5.3. Central modeling assumptions

Hydrogen demand. The HSC is designed to fulfill the regional hydrogen demands from refineries, ammonia production, methanol production, and other chemicals. In literature, hydrogen demand projections for

refineries, ammonia production, methanol production, and other chemicals for 2030 range from 233–312 TWh [6,16]. While the hydrogen demand from refineries is expected to decline and eventually vanish, the speed of this transition is uncertain. Depending on the scenario, hydrogen demand from refineries is expected to disappear by 2030 at the earliest and by 2050 at the latest. In contrast, the hydrogen demand from ammonia production and methanol production is assumed to remain similar to today's values or increase slightly (<3%) until 2050 [79]. Here, we assume that the hydrogen demands for refineries decline, and that the hydrogen demands from ammonia, methanol, and other chemicals remain stable until 2035. However, different demand projections can significantly impact the size and location of the installed hydrogen production and transport technologies. In particular, a shift in demand to locations with scarce renewable resources significantly increases the impact of spatial resolution (Section S8 [62]). We expect the impact of spatial resolution to heighten for larger hydrogen demands as the renewable energy potentials become increasingly constrained. Building upon this work, future studies could investigate the impact of varying hydrogen demand projections on the HSC design in further detail.

Biomass availability. Biomass-based hydrogen production technologies are identified as the most cost-efficient, low-hydrogen production technologies. Biomethane reforming and biomass gasification are deployed at a large scale, resulting in considerable biomass demands. In this work, the regional biomass availabilities are limited by the technical biomass potentials as described in Section 2.1. However, difficulties in biomass collection and a lack of infrastructure can reduce the realistically available biomass [106]. In addition, competing interests for biomass are not captured. Besides hydrogen production, biomass finds applications in the heating sector, the transport sector, and the electricity sector [107]. Hence, future work could consider uncertainty in the biomass availability and its impact on the optimal HSC design.

Temporal resolution. This work adopts a yearly time resolution. Similar to [18,34], we assume hydrogen demands from industry and the availability of dry- and wet-biomass to be constant throughout the year. The time-dependent capacity factors from wind- and solar energy are approximated by their average values. Thus, seasonality and intra-daily variability of wind and solar energy are not captured. As a result, the hydrogen production cost for electrolyzers powered with renewable electricity is likely underestimated. Hence, the temporal resolution of the optimization should be increased in HSC with large electrolysis capacities to account for their variable operation and the need for storage, as this likely results in an increase in the hydrogen production cost.

6. Conclusion

This work investigates the optimal design and infrastructure rollout of hydrogen supply chains (HSCs) to decarbonize the European hydrogen demand from refineries, ammonia production, methanol production, and other chemicals. We consider a multi-year time horizon from 2025–2035 and include several hydrogen production pathways, namely water-electrolysis with electricity, SMR with natural gas and biomethane, and biomass gasification. We investigate the coupling of hydrogen production with carbon capture and storage (CCS) when producing hydrogen from natural gas and biomass. In this context, carbon and biomass supply chains are designed alongside the HSC.

We investigate the impact of spatial resolution by comparing the levelized cost of hydrogen (LCOH), the optimal technology mix, and the optimal design of HSCs for different decarbonization targets, ranging from no decarbonization to full decarbonization by 2035. Two levels of spatial resolution are considered: regional (NUTS2) and national (NUTS0).

Independently of the spatial resolution, biomass-based hydrogen production is identified as the most cost-efficient, low-carbon hydrogen production technology. Replacing natural gas with biomethane reduces process emissions significantly and enables the transition from carbon-intensive, natural-gas-based hydrogen production to low-carbon hydrogen. Biomethane reforming is deployed at a large scale across all decarbonization targets. This measure is sufficient to realize decarbonization targets up to 30%. To achieve more ambitious decarbonization targets, biomass gasification is deployed; a more expensive but less carbon-intensive technology. Finally, the full decarbonization of the supply chains requires the coupling of biomass-based hydrogen production with CCS. Electrolysis is not found to be cost-competitive and only small capacities are deployed.

The results of the regional and national model are similar for decarbonization targets below 40 % in terms of cost. However, the impact of spatial resolution increases with increasing decarbonization targets, as fossil feedstocks are gradually replaced by renewable resources. By aggregating the hydrogen demands and the availability of the renewable resources, the national model underestimates transport costs and emissions, and fails to capture the need for a large-scale European hydrogen transport infrastructure. As a result, the levelized cost of hydrogen is underestimated. In fact, planning net-zero supply chains with a national resolution (NUTS0) might result in (i) a 31% cost increase compared to the regional designs (NUTS2), and (ii) an underestimation of the required transport infrastructure for hydrogen (by factor 7) and carbon (by factor 2), and an overestimation of the required dry biomass transport infrastructure (by a factor 2). In fact, without additional carbon removal technologies, planning net-zero supply chains with insufficient spatial resolution fail to achieve the decarbonization targets.

Overall, the findings highlight that spatial resolution is especially important when relying on large shares of spatially distributed renewable energy sources and when designing greenfield transport infrastructures. Considering high spatial resolutions unveils the relationship between interconnected infrastructures (here hydrogen, biomass, and carbon infrastructures), and the optimal placement of low-carbon hydrogen production sites, possibly impacting planning and road maps on national and European levels.

CRediT authorship contribution statement

Alissa Ganter: Conceptualization, Methodology, Software, Validation, Formal analysis, Investigation, Data curation, Writing – original draft, Visualization, Project administration. **Paolo Gabrielli:** Conceptualization, Methodology, Writing – review & editing, Supervision. **Giovanni Sansavini:** Conceptualization, Methodology, Resources, Writing – review & editing, Supervision, Funding acquisition.

Declaration of competing interest

The authors declare that they have no known competing financial interests or personal relationships that could have appeared to influence the work reported in this paper.

Code and data availability

The code and input data to reproduce the results presented in this work are available on Zenodo: https://doi.org/10.5281/zenodo.10568836.

Acknowledgments

The research published in this study was carried out with the support of the Swiss Federal Office of Energy (SFOE) as part of the SWEET PATHFNDR project. The authors bear sole responsibility for the conclusions and the results.

References

[1] European Comission. A hydrogen strategy for a climate-neutral Europe. Tech. Rep., European Comission; 2020, URL https://eur-lex.europa.eu/legal-content/EN/TXT/?uri=CELEX:52020DC0301.

[2] International Energy Agency (IEA). The future of hydrogen. Tech. Rep., International Energy Agency; 2019, URL https://iea.blob.core.windows.net/assets/9e3a3493-b9a6-4b7d-b499-7ca48e357561/The_Future_of_Hydrogen.pdf.

[3] Paltsev S, Morris J, Kheshgi H, Herzog H. Hard-to-Abate Sectors: The role of industrial carbon capture and storage (CCS) in emission mitigation. Appl Energy 2021;300(July):117322. http://dx.doi.org/10.1016/j.apenergy.2021.117322.

[4] Gabrielli P, Gazzani M, Mazzotti M. The role of carbon capture and utilization, carbon capture and storage, and biomass to enable a net-zero-CO2 emissions chemical industry. Ind Eng Chem Res 2020;59(15):7033–45. http://dx.doi.org/10.1021/acs.iecr.9b06579.

[5] Fonseca J, Muron M, Pawelec G, Yovchev IP, Kuhn M, Fraile D, et al. Clean hydrogen monitor. Tech. Rep., Hydrogen Europe; 2023, URL https://hydrogeneurope.eu/wp-content/uploads/2023/10/Clean_Hydrogen_Monitor_11-2023_DIGITAL.pdf.

[6] Fuel Cells and Hydrogen Joint Undertaking. Hydrogen roadmap europe: A sustainable pathway for the European energy transition. Tech. Rep., Fuel Cells and Hydrogen 2 Join Undertaking; 2019, p. 70. http://dx.doi.org/10.2843/249013, URL https://op.europa.eu/en/publication-detail/-/publication/0817d60d-332f-11e9-8d04-01aa75ed71a1.

[7] Fuel cells and hydrogen observatory. Hydrogen supply and demand. Tech. Rep., (September). Fuel Cells and Hydrogen Observatory; 2021, https://www.fchobservatory.eu/sites/default/files/reports/Chapter2HydrogenSupplyandDemand2021.pdf.

[8] Environmental Energy Agency (EEA). Annual European Union greenhouse gas inventory 1990–2020 and inventory report 2022. Tech. Rep., (May). Environmental Energy Agency; 2022, URL https://www.eea.europa.eu/publications/annual-european-union-greenhouse-gas-1.

[9] CertifHy. Hydrogen certification schemes. 2021, p. 1–4, URL https://www.certifhy.eu/go-labels/.

[10] Kakoulaki G, Kougias I, Taylor N, Dolci F, Moya J, Jäger-Waldau A. Green hydrogen in Europe – A regional assessment: Substituting existing production with electrolysis powered by renewables. Energy Convers Manage 2021;228:113649. http://dx.doi.org/10.1016/j.enconman.2020.113649, URL https://linkinghub.elsevier.com/retrieve/pii/S0196890420311766.

[11] Rosa L, Sanchez DL, Mazzotti M. Assessment of carbon dioxide removal potential via BECCS in a carbon-neutral Europe. Energy Environ Sci 2021;14(5):3086–97. http://dx.doi.org/10.1039/D1EE00642H, URL http://xlink.rsc.org/?DOI=D1EE00642H.

[12] European Clean Hydrogen Alliance. European electrolyzer summit. 2022, URL https://ec.europa.eu/docsroom/documents/50014/attachments/1/translations/en/renditions/native.

[13] European Hydrogen Observatory. Hydrogen pipelines. 2023, URL https://observatory.clean-hydrogen.europa.eu/hydrogen-landscape/distribution-and-storage/hydrogen-pipelines.

[14] European Commission. REPowerEU: Joint European action for more affordable, secure and sustainable energy EN. Tech. Rep., European Commission; 2022, URL https://eur-lex.europa.eu/legal-content/EN/TXT/?uri=COM:2022:108:FIN.

[15] Schlund D, Schulte S, Sprenger T. The who's who of a hydrogen market ramp-up: A stakeholder analysis for Germany. Renew Sustain Energy Rev 2022;154(November 2021):111810. http://dx.doi.org/10.1016/j.rser.2021.111810.

[16] Agora Energiewende and AFRY Management Consulting. No-regret hydrogen: Charting early steps for H2 infrastructure in Europe. Tech. Rep., Agora Energiewende and AFRY Management Consulting; 2021, URL https://www.agora-energiewende.de/en/publications/no-regret-hydrogen/.

[17] Wang A, David Mavins JJ, Moultak M, Schimmel M, Leun Kvd, Peters D, et al. Analysing future demand, supply, and transport of hydrogen. Tech. Rep., (June). European Hydrogen Backbone; 2021, URL https://gasforclimate2050.eu/wp-content/uploads/2021/06/EHB_Analysing-the-future-demand-supply-and-transport-of-hydrogen_June-2021.pdf.

[18] Neumann F, Zeyen E, Victoria M, Brown T. The potential role of a hydrogen network in Europe. Joule 2023. http://dx.doi.org/10.1016/j.joule.2023.06.016.

[19] Seck GS, Hache E, Sabathier J, Guedes F, Reigstad GA, Straus J, et al. Hydrogen and the decarbonization of the energy system in europe in 2050 : A detailed model-based analysis EU. Renew Sustain Energy Rev 2022;167(August):112779. http://dx.doi.org/10.1016/j.rser.2022.112779.

[20] Wulf C, Linssen J, Zapp P. Power-to-gas-concepts, demonstration, and prospects. Christina Wulf; 2018, p. 309–45. http://dx.doi.org/10.1016/B978-0-12-811197-0.00009-9.

[21] Parkinson B, Balcombe P, Speirs JF, Hawkes AD, Hellgardt K. Levelized cost of CO 2 mitigation from hydrogen production routes. Energy Environ Sci 2019;12(1):19–40. http://dx.doi.org/10.1039/C8EE02079E, URL http://xlink.rsc.org/?DOI=C8EE02079E.

[22] Bauer C, Treyer K, Antonini C, Bergerson J, Gazzani M, Gencer E, et al. On the climate impacts of blue hydrogen production. Sustain Energy Fuels 2022;6(1):66–75. http://dx.doi.org/10.1039/D1SE01508G, URL http://xlink.rsc.org/?DOI=D1SE01508G.

[23] Gabrielli P, Charbonnier F, Guidolin A, Mazzotti M. Enabling low-carbon hydrogen supply chains through use of biomass and carbon capture and storage: A Swiss case study. Appl Energy 2020;275:115245. http://dx.doi.org/10.1016/J.APENERGY.2020.115245.

[24] Glenk G, Reichelstein S. Economics of converting renewable power to hydrogen. Nat Energy 2019;4(3):216–22. http://dx.doi.org/10.1038/s41560-019-0326-1.

[25] International Renewable Energy Agency (IRENA). Green hydrogen cost reduction. Tech. Rep., IRENA; 2020, p. 105, URL https://www.irena.org/publications/2020/Dec/Green-hydrogen-cost-reduction.

[26] Antonini C, Treyer K, Streb A, van der Spek M, Bauer C, Mazzotti M. Hydrogen production from natural gas and biomethane with carbon capture and storage – A techno-environmental analysis. Sustain Energy Fuels 2020;4(6):2967–86. http://dx.doi.org/10.1039/D0SE00222D, URL http://xlink.rsc.org/?DOI=D0SE00222D.

[27] Antonini C, Treyer K, Moioli E, Bauer C, Schildhauer TJ, Mazzotti M. Hydrogen from wood gasification with CCS – a techno-environmental analysis of production and use as transport fuel. Sustain Energy Fuels 2021;5(10):2602–21. http://dx.doi.org/10.1039/D0SE01637C, URL http://xlink.rsc.org/?DOI=D0SE01637C.

[28] Rosa L, Mazzotti M. Potential for hydrogen production from sustainable biomass with carbon capture and storage. Renew Sustain Energy Rev 2022;157. http://dx.doi.org/10.1016/J.RSER.2022.112123.

[29] Shafiei E, Davidsdottir B, Leaver J, Stefansson H, Asgeirsson I. Comparative analysis of hydrogen, biofuels and electricity transitional pathways to sustainable transport in a renewable-based energy system. Energy 2015. http://dx.doi.org/10.1016/j.energy.2015.02.071.

[30] Moreno-Benito M, Agnolucci P, Papageorgiou LG. Towards a sustainable hydrogen economy: Optimisation-based framework for hydrogen infrastructure development. Comput Chem Eng 2017;102:110–27. http://dx.doi.org/10.1016/j.compchemeng.2016.08.005.

[31] Lepage T, Kammoun M, Schmetz Q, Richel A. Biomass-to-hydrogen: A review of main routes production, processes evaluation and techno-economical assessment. Biomass Bioenergy 2021;144(March 2020):105920. http://dx.doi.org/10.1016/j.biombioe.2020.105920.

[32] International Energy Agency (IEA). Technology perspectives energy special report on carbon capture utilisation and storage CCUS in clean energy transitions. Tech. Rep., International Energy Agency; 2020, URL https://iea.blob.core.windows.net/assets/181b48b4-323f-454d-96fb-0bb1889d96a9/CCUS_in_clean_energy_transitions.pdf.

[33] Meerman JC, Hamborg ES, van Keulen T, Ramírez A, Turkenburg WC, Faaij AP. Techno-economic assessment of CO2 capture at steam methane reforming facilities using commercially available technology. Int J Greenh Gas Control 2012;9:160–71. http://dx.doi.org/10.1016/j.ijggc.2012.02.018.

[34] Victoria M, Zeyen E, Brown T. Speed of technological transformations required in Europe to achieve different climate goals. Joule 2022;6(5):1066–86. http://dx.doi.org/10.1016/j.joule.2022.04.016.

[35] Won W, Kwon H, Han JH, Kim J. Design and operation of renewable energy sources based hydrogen supply system: Technology integration and optimization. Renew Energy 2017;103:226–38. http://dx.doi.org/10.1016/j.renene.2016.11.038.

[36] De-León Almaraz S, Azzaro-Pantel C, Montastruc L, Boix M. Deployment of a hydrogen supply chain by multi-objective/multi-period optimisation at regional and national scales. Chem Eng Res Des 2015;104:11–31. http://dx.doi.org/10.1016/J.CHERD.2015.07.005.

[37] Li L, Manier H, Manier MA. Hydrogen supply chain network design: An optimization-oriented review. Renew Sustain Energy Rev 2019;103(June 2018):342–60. http://dx.doi.org/10.1016/j.rser.2018.12.060.

[38] Almansoori A, Shah N. Design and operation of a future hydrogen supply chain: Snapshot model. Chem Eng Res Des 2006;84(6):423–38. http://dx.doi.org/10.1205/CHERD.05193.

[39] Almansoori A, Shah N. Design and operation of a future hydrogen supply chain: Multi-period model. Int J Hydrogen Energy 2009;34(19):7883–97. http://dx.doi.org/10.1016/j.ijhydene.2009.07.109, URL https://linkinghub.elsevier.com/retrieve/pii/S036031990901235X.

[40] Almansoori A, Shah N. Design and operation of a stochastic hydrogen supply chain network under demand uncertainty. Int J Hydrogen Energy 2012;37(5):3965–77. http://dx.doi.org/10.1016/j.ijhydene.2011.11.091.

[41] Struben J, Sterman JD. Transition challenges for alternative fuel vehicle and transportation systems. Environ Plan B: Plann Des 2008;35(6):1070–97. http://dx.doi.org/10.1068/B33022T.

[42] De-León Almaraz S, Azzaro-Pantel C, Montastruc L, Pibouleau L, Senties OB. Assessment of mono and multi-objective optimization to design a hydrogen supply chain. Int J Hydrogen Energy 2013;38(33):14121–45. http://dx.doi.org/10.1016/J.IJHYDENE.2013.07.059.

[43] Govindan K, Fattahi M, Keyvanshokooh E. Supply chain network design under uncertainty: A comprehensive review and future research directions. European J Oper Res 2017;263(1):108–41. http://dx.doi.org/10.1016/j.ejor.2017.04.009.

[44] Fazli-Khalaf M, Naderi B, Mohammadi M, Pishvaee MS. Design of a sustainable and reliable hydrogen supply chain network under mixed uncertainties: A case study. Int J Hydrogen Energy 2020;45(59):34503–31. http://dx.doi.org/10.1016/j.ijhydene.2020.05.276.
[45] Husarek D, Schmugge J, Niessen S. Hydrogen supply chain scenarios for the decarbonisation of a German multi-modal energy system. Int J Hydrogen Energy 2021;46(76):38008–25. http://dx.doi.org/10.1016/J.IJHYDENE.2021.09.041.
[46] Hwangbo S, Lee IB, Han J. Mathematical model to optimize design of integrated utility supply network and future global hydrogen supply network under demand uncertainty. Appl Energy 2017;195:257–67. http://dx.doi.org/10.1016/j.apenergy.2017.03.041.
[47] Fazeli R, Beck FJ, Stocks M. Recognizing the role of uncertainties in the transition to renewable hydrogen. Int J Hydrogen Energy 2022;47. http://dx.doi.org/10.1016/j.ijhydene.2022.06.122, 27896e27910.
[48] Tröndle T, Lilliestam J, Marelli S, Pfenninger S. Trade-offs between geographic scale, cost, and infrastructure requirements for fully renewable electricity in Europe. Joule 2020;4(9):1929–48. http://dx.doi.org/10.1016/j.joule.2020.07.018.
[49] Jalil-Vega F, Hawkes AD. The effect of spatial resolution on outcomes from energy systems modelling of heat decarbonisation. Energy 2018;155:339–50. http://dx.doi.org/10.1016/J.ENERGY.2018.04.160.
[50] Aryanpur V, O'Gallachoir B, Dai H, Chen W, Glynn J. A review of spatial resolution and regionalisation in national-scale energy systems optimisation models. Energy Strategy Rev 2021;37:100702. http://dx.doi.org/10.1016/J.ESR.2021.100702.
[51] Lopion P, Markewitz P, Robinius M, Stolten D. A review of current challenges and trends in energy systems modeling. Renew Sustain Energy Rev 2018;96:156–66. http://dx.doi.org/10.1016/j.rser.2018.07.045, URL https://linkinghub.elsevier.com/retrieve/pii/S1364032118305537.
[52] Martínez-Gordón R, Morales-España G, Sijm J, Faaij AP. A review of the role of spatial resolution in energy systems modelling: Lessons learned and applicability to the North Sea region. Renew Sustain Energy Rev 2021;141. http://dx.doi.org/10.1016/J.RSER.2021.110857.
[53] Pfenninger S, Hawkes A, Keirstead J. Energy systems modeling for twenty-first century energy challenges. Renew Sustain Energy Rev 2014;33:74–86. http://dx.doi.org/10.1016/J.RSER.2014.02.003.
[54] Hoffmann M, Kotzur L, Stolten D, Robinius M. A review on time series aggregation methods for energy system models. Energies 2020;13(3). http://dx.doi.org/10.3390/en13030641.
[55] Gabrielli P, Gazzani M, Martelli E, Mazzotti M. Optimal design of multi-energy systems with seasonal storage. Appl Energy 2018;219:408–24. http://dx.doi.org/10.1016/J.APENERGY.2017.07.142.
[56] Kotzur L, Markewitz P, Robinius M, Stolten D. Impact of different time series aggregation methods on optimal energy system design. Renew Energy 2018;117:474–87. http://dx.doi.org/10.1016/j.renene.2017.10.017.
[57] Horsch J, Brown T. The role of spatial scale in joint optimisations of generation and transmission for European highly renewable scenarios. In: International conference on the European energy market, EEM. 2017, p. 1–7. http://dx.doi.org/10.1109/EEM.2017.7982024.
[58] Krishnan V, Cole W. Evaluating the value of high spatial resolution in national capacity expansion models using ReEDS. In: IEEE power and energy society general meeting. 2016-Novem, IEEE; 2016, http://dx.doi.org/10.1109/PESGM.2016.7741996.
[59] Yliruka MI, Moret S, Jalil-Vega F, Hawkes AD, Shah N. The trade-off between spatial resolution and uncertainty in energy system modelling. In: Computer aided chemical engineering. vol. 49, Elsevier; 2022, p. 2035–40. http://dx.doi.org/10.1016/B978-0-323-85159-6.50339-0, URL https://linkinghub.elsevier.com/retrieve/pii/B9780323851596503390.
[60] Frew BA, Jacobson MZ. Temporal and spatial tradeoffs in power system modeling with assumptions about storage: An application of the POWER model. Energy 2016;117:198–213. http://dx.doi.org/10.1016/J.ENERGY.2016.10.074.
[61] Eurostat. Nomenclature of territorial units for statistics. 2023, URL https://ec.europa.eu/eurostat/web/nuts/overview.
[62] Ganter A, Gabrielli P, Sansavini G. Input data and code related to "Near-term infrastructure rollout and investment strategies for net-zero hydrogen supply chains". Dataset on Zenodo 2024. http://dx.doi.org/10.5281/zenodo.10568836.
[63] Capros P, De Vita A, Florou A, Kannavou M, Fotiou T, Siskos P, et al. EU reference scenario 2020. Tech. Rep., European Commission; 2021, p. 184, URL https://op.europa.eu/s/shWr.
[64] eurostat. Gas prices components for non-household consumers - annual data. 2022, URL https://ec.europa.eu/eurostat/databrowser/view/NRG_PC_203_CDEFAULTVIEW/default/table.
[65] Gonzalez-Aparicio I, Zucker A, Careri F, Monforti-Ferrario F, Huld T, Badger J. EMHIRES dataset: wind and solar power generation. Tech. Rep., Joint Research Centera; 2021, http://dx.doi.org/10.5281/zenodo.8340500, URL https://zenodo.org/records/8340501.
[66] Castello PR, Nijs W, Tarvydas D, Sgobbi A, Zucker A, Pilli R, et al. ENSPRESO - an open data, EU-28 wide, transparent and coherent database of wind, solar and biomass energy potentials. Tech. Rep., Joint Researc Center; 2019, http://data.jrc.ec.europa.eu/collection/id-00138 https://publications.jrc.ec.europa.eu/repository/handle/JRC116900.
[67] Kättlitz A, Cavarretta MC, Buyuk N, Lebois O, Boersma P. Scenario building guidelines. Tech. Rep., entsog and entso; 2021, URL https://2022.entsos-tyndp-scenarios.eu/wp-content/uploads/2022/04/TYNDP_2022_Scenario_Building_Guidelines_Version_April_2022.pdf.
[68] Scarlat N, Prussi M, Padella M. Quantification of the carbon intensity of electricity produced and used in Europe. Appl Energy 2022;305:117901. http://dx.doi.org/10.1016/j.apenergy.2021.117901.
[69] Ruiz P, Sgobbi A, Nijs W, Thiel C, Dalla Longa F, Kober T, et al. The JRC-EU-TIMES model - Bioenergy potentials for EU and neighbouring countries. Tech. Rep., Joint Research Center; 2015, p. 176. http://dx.doi.org/10.2790/39014, URL https://publications.europa.eu/en/publication-detail/-/publication/b291a7c5-a878-11e5-b528-01aa75ed71a1/language-en.
[70] International Energy Agency (IEA). IEA G20 hydrogen report: Assumption. Tech. Rep., IEA; 2020, URL https://iea.blob.core.windows.net/assets/29b027e5-fefc-47df-aed0-456b1bb38844/IEA-The-Future-of-Hydrogen-Assumptions-Annex_CORR.pdf.
[71] Sgobbi A, Nijs W, De Miglio R, Chiodi A, Gargiulo M, Thiel C. How far away is hydrogen? Its role in the medium and long-term decarbonisation of the European energy system. Int J Hydrogen Energy 2016;41(1):19–35. http://dx.doi.org/10.1016/j.ijhydene.2015.09.004.
[72] Terlouw W, Peters D, van der Leun K. Gas for Climate. The optimal role for gas in a net zero emissions energy system. Tech. Rep., Navigant; 2019, URL https://gasforclimate2050.eu/wp-content/uploads/2020/03/Navigant-Gas-for-Climate-The-optimal-role-for-gas-in-a-net-zero-emissions-energy-system-March-2019.pdf.
[73] COMTECSWISS. CO2-ISO CONTAINER. 2022, URL http://www.comtecswiss.com/en/equipment-and-plants/co2-iso-container/.
[74] Reuß M, Grube T, Robinius M, Stolten D. A hydrogen supply chain with spatial resolution: Comparative analysis of infrastructure technologies in Germany. Appl Energy 2019;247(December 2018):438–53. http://dx.doi.org/10.1016/j.apenergy.2019.04.064.
[75] Becattini V, Gabrielli P, Antonini C, Campos J, Acquilino A, Sansavini G, et al. Carbon dioxide capture, transport and storage supply chains: Optimal economic and environmental performance of infrastructure rollout. Int J Greenh Gas Control 2022;117:103635. http://dx.doi.org/10.1016/j.ijggc.2022.103635, URL https://linkinghub.elsevier.com/retrieve/pii/S1750583622000548.
[76] Agency for the Cooperation of Energy Regulators (ACER). Transporting Pure Hydrogen by Repurposing Existing Gas Infrastructure: Overview of existing studies and reflections on the conditions for repurposing. Tech. Rep., ACER; 2021, https://acer.europa.eu/Official_documents/Acts_of_the_Agency/Publication/TransportingPureHydrogenbyRepurposingExistingGasInfrastructure_Overviewofstudies.pdf.
[77] Reuß M, Grube T, Robinius M, Preuster P, Wasserscheid P, Stolten D. Seasonal storage and alternative carriers: A flexible hydrogen supply chain model. Appl Energy 2017;200:290–302. http://dx.doi.org/10.1016/j.apenergy.2017.05.050, URL https://linkinghub.elsevier.com/retrieve/pii/S0306261917305457.
[78] Krasae-in S, Stang JH, Neksa P. Development of large-scale hydrogen liquefaction processes from 1898 to 2009. Int J Hydrogen Energy 2010;35(10):4524–33. http://dx.doi.org/10.1016/j.ijhydene.2010.02.109.
[79] Material Economics. Industrial transformation 2050 - pathways to net-zero emissions from EU heavy industry. Focus Catal 2019;2006(12):8, URL https://materialeconomics.com/publications/industrial-transformation-2050.
[80] European Hydrogen Observatory. Hydrogen production. 2022, URL https://observatory.clean-hydrogen.europa.eu/hydrogen-landscape/production-trade-and-cost/hydrogen-production.
[81] Wachsmuth J, Aydemir A, Döscher H, Eckstein J, Proganietz W, Francois DE, et al. The potential of hydrogen for decarbonising EU industry. Tech. Rep., European Parliamentary Research Service Scientific Foresight Unit (STOA) PE 697.199 – December 2021; 2021, http://dx.doi.org/10.2861/271156, URL https://www.europarl.europa.eu/RegData/etudes/STUD/2021/697199/EPRS_STU(2021)697199_EN.pdf.
[82] Equinor. Northern lights project concept report. Tech. Rep., Equinor; 2019, p. 1–139, URL https://norlights.com/wp-content/uploads/2021/03/Northern-Lights-Project-Concept-report.pdf.
[83] ZEP. The costs of CO2 capture, transport and storage - post-demonstration CCS in the EU. 2011, URL https://www.zeroemissionsplatform.eu/library/publication/168-zep-cost-report-storage.html.
[84] Deng H, Roussanaly S, Skaugen G. Techno-economic analyses of CO 2 liquefaction: Impact of product pressure and impurities. 2019, http://dx.doi.org/10.1016/j.ijrefrig.2019.04.011.
[85] Schnorf V, Trutnevyte E, Bowman G, Burg V. Biomass transport for energy: Cost, energy and CO2 performance of forest wood and manure transport chains in Switzerland. J Clean Prod 2021;293:125971. http://dx.doi.org/10.1016/j.jclepro.2021.125971, URL https://linkinghub.elsevier.com/retrieve/pii/S0959652621001918.
[86] Scarlat N, Fahl F, Dallemand JF, Monforti F, Motola V. A spatial analysis of biogas potential from manure in Europe. Renew Sustain Energy Rev 2018;94:915–30. http://dx.doi.org/10.1016/J.RSER.2018.06.035.
[87] Gurobi Optimization LLC. Gurobi optimizer reference manual. 2022, URL https://www.gurobi.com.

[88] National Renewable Energy Laborotary (NREL). Simple levelized cost of energy (LCOE) calculator documentation | energy analysis | NREL. 2022, p. 1, URL https://www.nrel.gov/analysis/tech-lcoe-documentation.html.

[89] Konstantin P, Konstantin M. Power and energy systems engineering economics. Springer International Publishing AG; 2018, http://dx.doi.org/10.1007/978-3-319-72383-9.

[90] European Commission. 'Fit for 55': delivering the EU's 2030 Climate Target on the way to climate neutrality. Tech. Rep., European Comission; 2021, URL https://eur-lex.europa.eu/legal-content/EN/TXT/?uri=CELEX%3A52021DC0550.

[91] Seront X, Fernandez R, Qoul C, Gugele B, Righler E. Annual European Union greenhouse gas inventory 1990–2021 and inventory report 2023. Tech. Rep., (April). European Environment Agency; 2023, URL https://www.eea.europa.eu/publications/annual-european-union-greenhouse-gas-2.

[92] IPCC. Carbon dioxide capture and storage. Tech. Rep., Cambridge University Press; 2005, http://dx.doi.org/10.1016/bs.ache.2021.10.005, URL https://www.ipcc.ch/report/carbon-dioxide-capture-and-storage/.

[93] climeworks. Support the scale - up of direct air capture. 2023, p. 1–9, URL https://climeworks.com/subscriptions.

[94] Statista. European Union Emission Trading System (EU-ETS) carbon pricing in 2022. 2022, URL https://www.statista.com/statistics/1322214/carbon-prices-european-union-emission-trading-scheme/.

[95] International Energy Agency (IEA). Energy technology perspectives 2020 - special report on carbon capture utilisation and storage. 2020, http://dx.doi.org/10.1787/208b66f4-en.

[96] Department for Business Energy & Industrial Strategy (DBEIS). Hydrogen production costs 2021. Tech. Rep., (August). UK Department for Business Energy & Industrial Strategy; 2021, URL https://www.iea.org/data-and-statistics/charts/hydrogen-production-costs-by-production-source-2018.

[97] International Energy Agency (IEA). World energy model – documentation. Tech. Rep., International Energy Agency (IEA); 2020, URL https://www.iea.org/reports/world-energy-model.

[98] European Commission. Communication COM/2020/301: A hydrogen strategy for a climate-neutral Europe. Tech. Rep., 53, (9). Brussels: European Commission; 2020, URL https://eur-lex.europa.eu/legal-content/EN/TXT/?uri=CELEX:52020DC0301.

[99] European commission. Implementing REPowerEU Plan. RePowerEU plan 2022. URL https://eur-lex.europa.eu/legal-content/EN/TXT/PDF/?uri=CELEX:52022SC0230&from=EN.

[100] Odenweller A, Ueckerdt F, Nemet GF, Jensterle M, Luderer G. Probabilistic feasibility space of scaling up green hydrogen supply. Nat Energy 2022;7(9):854–65. http://dx.doi.org/10.1038/s41560-022-01097-4, URL https://www.nature.com/articles/s41560-022-01097-4.

[101] Blanco H, Gómez Vilchez JJ, Nijs W, Thiel C, Faaij A. Soft-linking of a behavioral model for transport with energy system cost optimization applied to hydrogen in EU. Renew Sustain Energy Rev 2019;115:109349. http://dx.doi.org/10.1016/J.RSER.2019.109349.

[102] Biggins F, Kataria M, Roberts D, Brown DS. Green hydrogen investments: Investigating the option to wait. Energy 2022;241:122842. http://dx.doi.org/10.1016/j.energy.2021.122842.

[103] Lane B, Reed J, Shaffer B, Samuelsen S. Forecasting renewable hydrogen production technology shares under cost uncertainty. Int J Hydrogen Energy 2021;46(54):27293–306. http://dx.doi.org/10.1016/J.IJHYDENE.2021.06.012.

[104] Ueckerdt F, Verpoort P, Anantharaman R, Bauer C, Beck F, Longden T, et al. On the cost competitiveness of blue and green hydrogen. SSRN Electron J 2023;(1). http://dx.doi.org/10.2139/ssrn.4501786, URL https://papers.ssrn.com/sol3/papers.cfm?abstract_id=4501786.

[105] van Rossum R, Jens J, La Guradia G, Wang A, Kühnen L, Overgaag M. European hydrogen backbone: A European hydrogen infrastructure vision covering 28 countries. Tech. Rep., (April). Guidehouse; 2022, URL https://ehb.eu/Page/European-Hydrogen-Backbone-Maps.

[106] Nevzorova T, Kutcherov V. Barriers to the wider implementation of biogas as a source of energy: A state-of-the-art review. Energy Strategy Rev 2019;26:100414. http://dx.doi.org/10.1016/j.esr.2019.100414.

[107] Wu F, Muller A, Pfenninger S. Strategic uses for ancillary bioenergy in a carbon-neutral and fossil-free 2050 European energy system. Environ Res Lett 2023;18(1). http://dx.doi.org/10.1088/1748-9326/aca9e1.